Indium tin oxide thin film preparation and property relationship for humidity sensing: a review.

RAJENDRAN, V., PRATHURU, A., FERNANDEZ, C., SUJATHA, D., PANDA, S.K. and FAISAL, N.H.

2024

Indium tin oxide thin film preparation and property relationship for humidity sensing: A review

Vinooth Rajendran¹ | **Anil Prathuru¹** | **Carlos Fernandez²** | **Dhavamani Sujatha³,⁴** | **Subhendu K. Panda³,⁴** | **Nadimul Haque Faisal¹**

¹School of Engineering, Robert Gordon University, Aberdeen, UK

²School of Pharmacy and Life Sciences, Robert Gordon University, Aberdeen, UK

³Electroplating and Metal Finishing Division, CSIR – Central Electrochemical Research Institute (CECRI), Karaikudi, India

⁴Academy of Scientific & Innovative Research (AcSIR), Ghaziabad, India

Correspondence
Nadimul Haque Faisal, School of Engineering, Robert Gordon University, Garthdee Road, Aberdeen, AB10 7GJ, UK.
Email: n.h.faisal@rgu.ac.uk

Abstract

This review aims to present a critical overview of indium tin oxide (ITO) thin film preparation methods, structure–property relationship, and its humidity sensing. A range of passive and active humidity sensors with thin films (based on metal oxides) detects humidity. ITO thin film has advantageous properties, such as low resistivity and high stability, making it highly suitable for humidity sensing applications. ITO thin film has shown the efficient level of humidity sensing, and a compatible size of humidity sensor can monitor the interface conditions humidity. So far, the application of ITO thin film for humidity measurement has yet to be explored at commercial scale, specifically in the detection of lower environmental humidity range (below 5% relative humidity (RH)). The research reveals a gap in improving the ITO thin film properties with an optimal range of preparation conditions. The research opportunities in the preparation, properties, characteristics, and efficient humidity sensitivity of ITO thin film are reviewed in this work.

KEYWORDS
annealing temperature, humidity sensing, indium tin oxide (ITO), thickness, thin film

1 | INTRODUCTION

Indium tin oxide (ITO) is a transparent semiconducting material with the advantages of electrical conductivity, low resistivity, and high optical transmittance in the visible region, along with a wide bandgap ranging from 3.5 to 4.3 eV, and with good chemical stability. ITO has various applications such as antistatic applications, architectural coatings, transparent electrodes in solar cells and flat panel displays, gas sensors, organic light-emitting diodes (OLED), and humidity sensing. There are several methods to prepare ITO thin films, each with specific advantages and limitations. ITO thin film properties are directly related to the preparation conditions. During preparation, mainly it depends on the annealing and substrate temperature, tin concentration, and thin film thickness. Research on ITO thin film humidity measurement has been ongoing for over a decade. A critical evaluation reveals that there is still an opportunity to enhance ITO thin film properties and its humidity sensing efficiency.

ITO thin films have been prepared using various methods, such as dip coating method,[1–7] DC magnetron sputtering,[8–14] radio frequency (RF) sputtering,[15–24] spin coating,[25–34] direct and thermal evaporation,[35–37] electron beam (EB) evaporation,[38–42] pulsed laser deposition (PLD),[43–45] chemical vapor deposition,[46,47] microwave heating,[48,49] screen-printed process,[50–56] and spray pyrolysis method.[57–59]

Critical assessment of the methodologies indicates that ITO thin film properties are highly dependent on the multiple preparation processes conditions such as substrate temperature, deposition rate, substrate pre-preparation, tin concentration, oxygen partial pressure, and annealing temperature, which are discussed below in much detail.[11,15] Arguably, the crystalline structure of ITO has a significant influence on ITO thin film properties and performance. Typically, a stabilizer is used which is an additive to preserve the crystalline structure, and a binder used which is an agent to enhance the adhesion of the material. For example, Dong et al.[27] proposed a new approach of using oxalic acid as a stabilizer, methylcellulose as binder, and post thermal treatment at 500°C applied to improve the conductivity and transmittance of ITO thin film. Analysis indicated that the thin film resistivity decreases through an annealing process. Additionally, the low resistivity of the thin film could be generated by increased oxygen vacancies and substitutional tin dopants on indium.[59,60] It has been suggested that the deposition rate plays a critical role in determining the ITO thin film quality, and the resistivity of thin films linearly increases with the deposition rate. A low deposition rate promotes crystalline phase formation,[61] whereas a high deposition rate by the sputtering method causes thermal damage to the substrate. As an example, Hoshi et al.[62] used sputtering to minimize the substrate's thermal damage at a high deposition rate. ITO is a highly promising material for high-temperature thin film sensor applications. ITO thin films, when coated on alumina substrates, underwent thermal cycle tests from 500°C to 1200°C. After the thermal tests, the morphology results showed a smoother surface with no cracks or pinholes. Additionally, recrystallization of these films improved the average grain size.[63]

Various active and passive humidity sensors are available to monitor humidity in a range of applications such as agriculture, predictive maintenance, instrumentation, healthcare, automation, climate monitoring, food-quality preservation, and domestic applications (Figure 1).[64–67] To meet the demands for humidity measurements, it required the further development of cost-effective, high-performance sensors, the establishment of innovative sensing modes, process technologies, and incorporation of new materials to provide cheaper, a wide dynamic range, and quick response time.[65] The development of advanced ITO thin films with high humidity sensing properties is highly necessary for various industries, particularly for effective monitoring of interface conditions and low humidity levels. Compared to other humidity sensing materials, ITO thin film can offer better humidity sensing with its advantageous properties. The preparation of advanced ITO thin films and compact sensor design could provide an opportunity for economically effective humidity monitoring. Various metal oxides such as graphene oxide (GO), zinc oxide (ZnO), zirconium dioxide (ZrO_2), barium oxide (BaO), and tin oxide (SnO_2) have been considered for different humidity sensing applications. GO is a highly promising humidity sensing material and showed excellent physical properties of mechanical stiffness (130 GPa), thermal conductivity (4.84×10^3 W mK^{-1} to 5.30×10^3 W mK^{-1}), large surface specific area (2600 m^2 g^{-1}), carrier mobility (200,000 cm^2 V^{-1}), bandgap (2.2 eV), and electrical and optical properties. Inkjet printing deposited GO layer could perform with a quick response (2.7 s) and recovery (4.6 s) time with a humidity range of 11%–97%.[68,69] An advanced form of the ZnO (in the nanostructure form) has shown high-level humidity sensing properties, a bandgap of 3.37 eV, and high thermal and mechanical stability at room temperatures.[70,71]

ZrO_2 is an ideal ceramic material with various practical applications such as catalysis, as optical devices, as fuel cell electrolytes, including humidity sensing.[72] Hydrothermal synthesis is a unique method to synthesize ZrO_2 nanoparticles with high purity and controlled microstructures, which could be a better option to enhance the properties. The ZrO_2 samples with high surface proportions provides high oxygen absorption and high humidity sensitivity.[73] Agool, Kadhim and Hashim[74] studied nanocomposites of polyvinyl alcohol-polyethylene glycol-polyvinyl pyrrolidone (PVA-PEG-PVP) blend with ZrO_2 nanoparticles as an additive for humidity sensing. ZrO_2 (weight: 0%, 2%, 4%, 6%, 8%) mixed with the PVA (90 wt.%), PEG (5 wt.%), and PVP (5 wt.%). Analysis showed that the resistance decreases with increasing relative humidity for all nanocomposites thin films. The absence of ZrO_2 nanoparticle thin film showed a higher resistance with relative humidity at room temperature. Sathya[75] designed the humidity sensor thin film of Al_2O_3 on the ZrO_2 and measured the humidity from 10% to 90% RH with an average sensitivity of 2.226.

Barium oxide (BaO) has a unique wide energy bandgap (3.8 eV) compared to other metal oxides, and the humidity sensing performance of BaO nanoparticles (measured through DC resistance method) with relative humidity (RH)
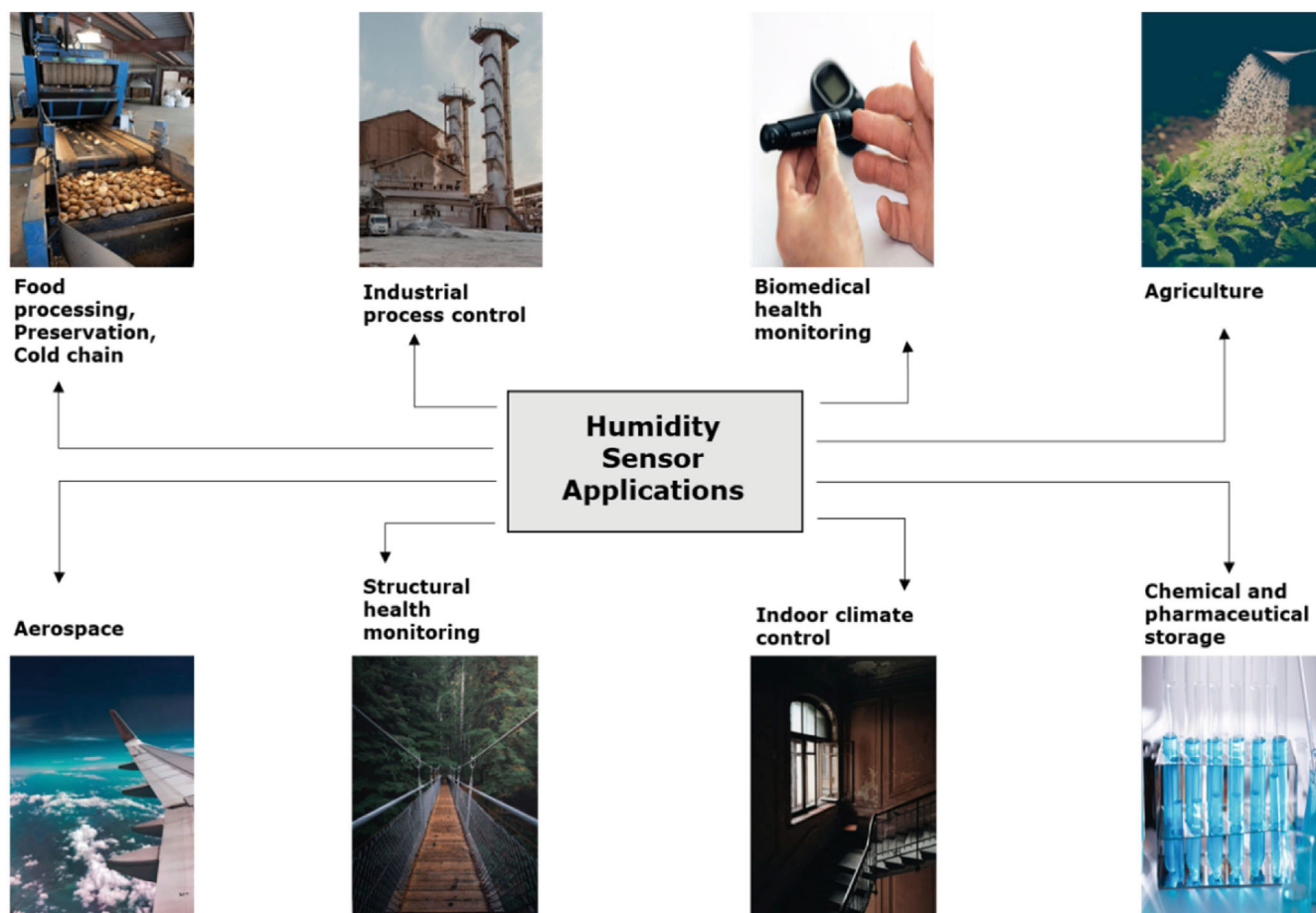
FIGURE 1 Diverse application of humidity sensors (representative examples) (permissions not needed for these images, attribution is not required).

ranging from 5% to 98% at room temperature. It showed linear resistance behavior with relative humidity. The result confirmed the quick response and recovery time of the 40 and 110 s, respectively.[76] SnO_2 is a rutile structure and n-type semiconducting material with a bandgap of 3.6 eV at 300 K, with good electrical and optical properties, and high chemical stability.[77] Parthibavarman, Hariharan and Sekar[78] deposited SnO_2 nanoparticles using microwave irradiation technique. The relative humidity raised from 5% to 95%, increasing the conductivity and reducing the resistance, and it showed the response and recovery time of 32 and 25 s, respectively. Li, Li and Zhang[79] designed a high-performance humidity sensor (zinc oxide/tin oxide (ZnO/SnO_2)) with low-cost metal oxide of tin oxide by using the solvothermal method. SnO_2 enhanced the humidity absorption, and ZnO improved the oxygen-rich vacancies on the composite thin film, allowing for the absorption of the water molecules and speeding up the ionization, increasing the response and recovery time performance. ZnO/SnO_2 humidity sensor showed the 35 and 8 s of response and recovery time in the humidity range of 11%–95%. Each humidity sensing materials has advantageous properties and limitations for humidity sensing. These limitations can be overcome through further development in preparation and sensor design.

This review has attempted to critically evaluate ITO thin film preparation methods, the effect of the processing conditions, structure–property relationships, and humidity sensing. Previous literature studies covered the ITO thin film humidity sensing of humidity ranging from 5% RH to 98% RH, including those yet to explore below 5% RH level measurement. An appropriate condition for humidity measurement of ITO thin film preparation still needs to be discovered. Assessing the impact of such materials, fabricating an improved ITO thin film with humidity sensing applications, and improving sensitivity from low to high relative humidity can prevent humidity-related accidents and economic losses in industries.

2 | ITO THIN FILM PREPARATION

Various preparation methods are available to prepare ITO thin film based on each method's unique advantages and limitations. For example, thin film resistivity and transmittance changes based on the preparation methods such as EB evaporation (3.0×10^{-6} Ωm, 92%), reactive evaporation (7.0×10^{-6} Ωm, 80%), PLD (4.0×10^{-6} Ωm, 85%), thermal deposition (9.1×10^{-6} Ωm, 80%), and DC magnetron sputtering (4.0×10^{-5} Ωm, 97%).[39] Based on published literature, Figure 2 presents ITO thin film preparation methods (various approaches). The process steps involved in the synthesis of ITO thin film preparation highly depend on preparation conditions and the substrate used. The synthesis process is important for determining the quality and characteristics of the ITO thin film. The relationship between the concentration of tin, deposition method, substrate, and annealing temperature with the characterization of the ITO thin film is reviewed below. Particularly, the selection of the substrate depends on the application, deposition method, and temperature levels. Generally, the substrates are cleaned ultrasonically in acetone, rinsed in water, and dried in an oven before deposition begins. The solutions are prepared through different procedures based on the deposition method, with continuous stirring for a certain duration, followed by the addition of other agents (i.e., capping, precipitate agent) to enhance solution quality, bonding between the substrate and thin film, and extend the service life of the thin film.

Nishio Sei and Tsuchiya[80] demonstrated the successful deposition of an ITO thin film on a quartz glass substrate using a dip coating process. The substrate was directly dipped into an ITO solution, and then heat treatment was carried to enhance crystallization during the dip coating process. Though still challenging, advantages of the dip-coating process included its cost-effectiveness and the ability to deposit multiple layers through repeated heating and dipping processes. The stability and sensitivity of dip-coated thin films were suitable for sensing applications of gas and humidity.[4,5] Sputtering has been frequently used to deposit the ITO thin film to obtain high conductivity at low substrate temperature deposition. The dip-coating fabrication could be used to deposit ITO thin film on a large area at a low cost, although the film's conductivity may generally be lower than that achieved through sputtering.[3]
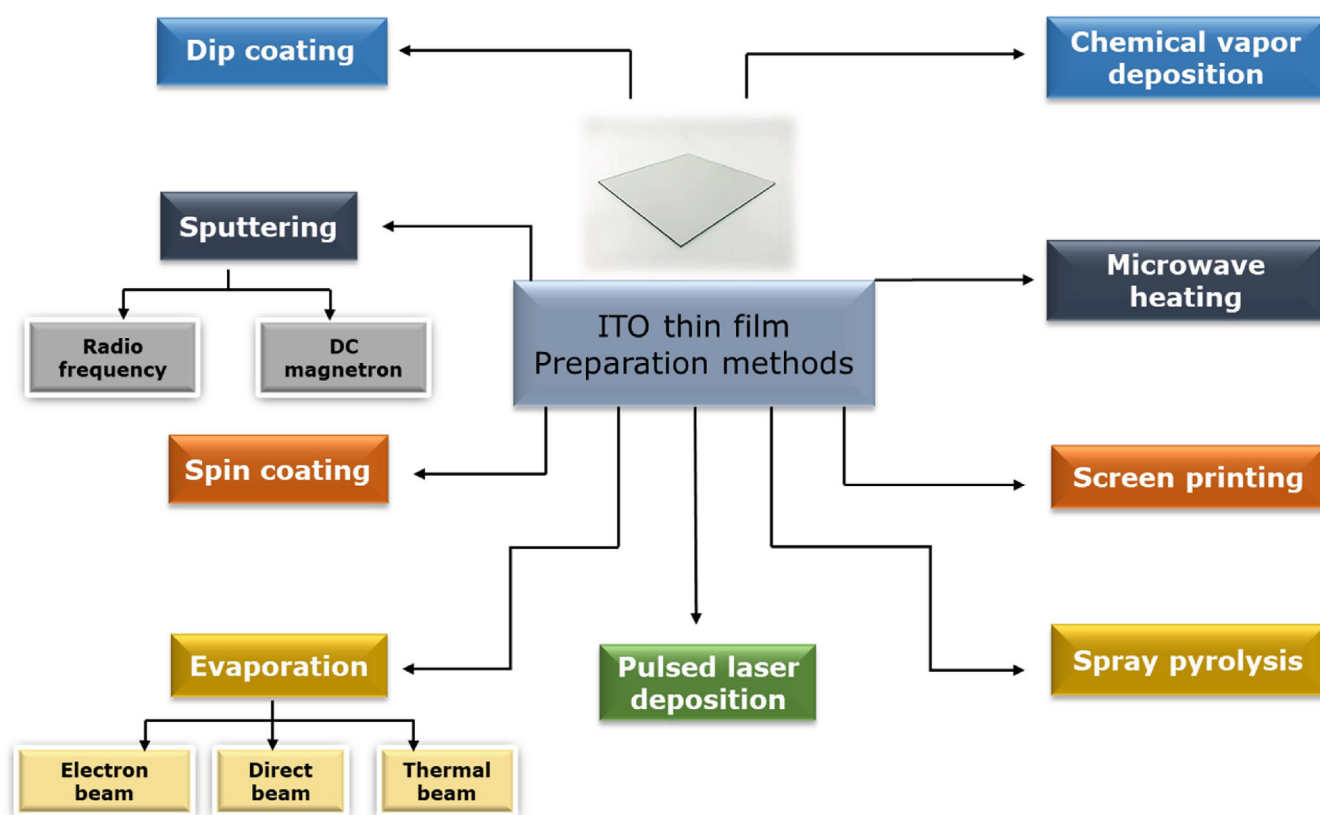

FIGURE 2 Types of ITO thin film fabrication methods (authors original images).

Many years ago, Almeida[81] discussed the fundamental physics and design of DC sputtering. In recent times, ITO thin films have been fabricated by DC magnetron sputtering, starting from room temperature to 400°C on to a glass substrate.[9,10] However, DC magnetron sputtering of conductive oxide material has been frequently accompanied by an electric arc as a form of electric breakdown, and the electric breakdown mostly appeared on the target substrate. This issue can be overcome by using a pulsed DC magnetron sputtering system.[8] El Akkad et al.[17] investigated the deposition of ITO thin films by radio frequency (RF) sputtering method. RF sputtering allows thin film deposition from room temperature to 230°C, with varying deposition rates.[21] Compared to the other available deposition methods, DC magnetron sputtering is commonly used method for good film preparation and has been available for large industrial production.[11] However, it requires high-cost vacuum equipment, which is considered a disadvantage. Another disadvantage of sputtering is a high surface roughness at room temperature deposition. Thin films with high surface roughness are generally unsuitable for many applications, especially humidity sensing, as high surface roughness can reduce humidity measurement sensitivity,[5] primarily due to reduced contact area, and slower response time due to trapped air in small crevices.

Kim et al.[29] considered preparing ITO thin film on a glass substrate at room temperature by sol–gel spin coating. It was demonstrated that a repeated process could be beneficial to make a multilayer deposition, with decreased surface roughness and film resistance.[82] Various methods have been applied to prepare spin coating solution with different concentration levels. Spin coating is a beneficial method for thin film preparation with the required shape and size. In such method, the doping level and concentration of a solution could be controlled easily. Moreover, it is cost-effective and yields stable, uniform, and robust films with better reproducibility by a simple process. The uniformity of thin film is confirmed by SEM images as demonstrated by Babu and Vadivel.[25] Sofi, Shah, and Asokan[35] fabricated ITO thin films on glass substrate by thermal evaporation technique, followed by oxidation for 15 min in atmosphere in temperature range of 600°C–700°C. Followed by surface morphology analysis carried out by using SEM. The results showed that, thin film is uniform and good adherence with glass substrate without any defects like cracks, voids, and pinholes within the grains. With these advantages, Singh et al.[83] synthesized nanomaterial ITO thin film layers on a glass substrate by adding a dilute solution to the substrate, which spun at 3000 rpm for 60 s. The results showed advanced materials characterization of ITO thin film via spin coating, supported by the presence of indium doped SnO_2 nanomaterial.

Multiple types of evaporation techniques, such as thermal, direct and electron evaporation, have been applied to deposit ITO thin film on glass substrates. George and Menon[39] considered ITO thin film deposition by the EB evaporation technique. Patel, Makhija and Panchal[84] fabricated the ITO thin film on the alumina substrate through thermal evaporation. Evaporation techniques are known for their effectiveness in producing high-quality thin films. In these techniques, deposition control is achieved by adjusting the oxygen pressure during the process.[40,41] It is worth noting that ITO thin films prepared using evaporation methods typically require high temperatures, which can be considered one of their limitations.[36] Kim et al.[85] grew the ITO thin film on a glass substrate by PLD. Craciun et al.[44] deposited a high-quality ITO thin film at temperature range from 40°C to 180°C on glass and silicon substrate using ultraviolet-assisted pulsed laser deposition (UVPLD). The average thickness of these films was 150 mm. However, the same thickness of thin film (i.e., 150 mm) can be achieved through PLD at a temperature of 300°C.

Maruyama and Fukui[47] prepared ITO thin film on a glass substrate by chemical vapor deposition (CVD) in an electric furnace without using an oxygen donor. Atmospheric pressure chemical vapor deposition (AP-CVD) offered a simple process to do deposition on a large area compared to the other methods. It did not require any specific vacuum condition or coating chamber to do a process, resulting the cost lower for thin film production.[46]

Microwave heating is a unique way to produce thin film with low resistance and high optical transparency in few minutes. Rapid thermal annealing (RTA) is a well-known process to reduce mechanical damage and diffuse impurities within thin film compared to long time annealing and heat-treatment processes. Microwave heating operates similar to RTA. In such process, the prepared ITO solution can be applied and dried at 80°C on to a glass substrate. The glass plate can then undergo quick microwave irradiation. The microwave irradiation at 2.5 GHz was conducted using a commercial microwave with a power output of 700 W. Through such microwave heating process, ITO thin films can be deposited 5 times repeatedly on a glass substrate to achieve thickness of 900 nm. The advanced approach of microwave enhanced reactive magnetron sputtering could help to avoid oxidation of the sample during sputtering.[48,49]

Screen print has an advantage that it could be printed on selected or specific areas. Bessais, Ezzaouia and Bennaceur[51] prepared the ITO thin film on glass and silicon substrate by screen printing technique. McGhee et al.[12,50] printed ITO on the PET substrate, which was cured in the oven at 105°C before applying alumina ink on top. Subsequently, the final ITO thin film was printed on top of the alumina ink and cured for 5 min at 105°C. The analysis demonstrated that the alumina dielectric ink was effective in preventing short circuits between the two ITO layers. Siddiqui, Saxena and Singh[86] performed screen printing to deposit silver bus bars on the edges of glass substrate and followed by the deposition of ITO through sputtering on remaining areas.

Benamar et al.[87] investigated the electrical, structural, and optical properties of ITO thin films prepared by spray pyrolysis on a glass substrate. ITO thin films were deposited on the glass substrate by spray pyrolysis with different solution concentration levels at a substrate temperature of 500°C. It was demonstrated that the film's adherence depends on the substrate, transparency, and pinhole free. Marikkannu et al.[58] prepared ITO thin films by the JNS pyrolysis technique on heated glass and porous silicon substrate at a 350°C–450°C temperature. The air pressure was 3.5 kg cm^{-2}, the distance of the nozzle from the substrate was 5 cm, and rate of spray was 0.75 mL min^{-1}. The spray continued for 10 mins on both substrates.

Some recent study highlights the advantages of using a glass substrate as the base structure. ITO thin films on polyethylene terephthalate (PET) and glass substrates have been investigated for the CO_2 reduction reaction in water vapor. According to the manufacturer's information, the thickness of the ITO thin film on the glass substrate ranged from 30 nm to 60 nm, while the PET substrate of 130 nm thickness. Analysis revealed that the ITO glass substrate exhibited a lower peak intensity compared to the ITO-PET substrate. This lower intensity indicates more efficient electron/hole separation on the ITO glass substrate compared to the ITO-PET substrate, suggesting a higher number of charge carriers in the ITO glass. The XRD pattern of the ITO glass substrate showed a peak corresponding to the cubic In_2O_3 structure, whereas the XRD pattern of the ITO-PET substrate did not exhibit the ITO structure.[88]

In summary, the polymer substrate had the advantages of being lightweight and having higher shock resistance. However, the high temperature of thin film preparation and heat treatment can lead to the polymer substrate decomposition, releasing toxic compounds. It is important to note that structural degradation can introduce microcracks in ITO thin film.[19] Overall, it has been demonstrated that the glass substrate is more appropriate for ITO thin film fabrication compared to the polymer substrate due to the glass substrate can withstand higher temperatures without any structural decomposition and failure. Overall, various literature demonstrated that the spin coating method has the advantage of low cost, efficiently controlled doping level, simplicity, and flexibility in preparing large and small sizes of thin films. In recommendation, spin coating is more appropriate to prepare ITO thin film in lab scale. The preparation conditions relationship with thin film properties is discussed below.

3 | ITO THIN FILM PROPERTIES AND PREPARATION DEPENDENCIES

Based on a critical review of ITO thin film preparation methods, along with their challenges and advantages, it has become evident that ITO thin film properties are highly dependent on various thin film preparation conditions, particularly including annealing and substrate temperature, tin concentration, and thin film thickness. Thin film's parameters such as resistivity, surface roughness, grain size, crystalline structure, banggap, and transmittance are interconnected with preparation conditions. The relationship between preparation conditions and thin film parameters are critically reviewed here. An improved ITO thin film properties can be achieved through selection of appropriate preparation conditions. Figure 3 illustrates the thin film properties' connection with the fabrication parameters. Modifications in preparation conditions directly influence thin film properties and humidity sensing behavior, as discussed below.

3.1 | Annealing temperature

The annealing process is essential for enhancing resistivity behavior, transmittance, bandgap, carrier concentration, carrier mobility, and grain size of ITO thin films. Typically, the annealing temperature range from 200°C to 700°C, and annealing time duration depends on the applications of the thin film. An annealing process promotes the transformation from amorphous to a polycrystalline structure, with oxygen vacancies enhancing conductivity.

Ota et al.[3] deposited ITO thin film by dip coating on a glass substrate (Corning #7059, 25 mm × 37 mm × 0.7 mm). The coated substrate was annealed at 600°C for 1 h with a heating rate of 10°C min^{-1} and N_2-0.1% H_2 flow rate. As a result
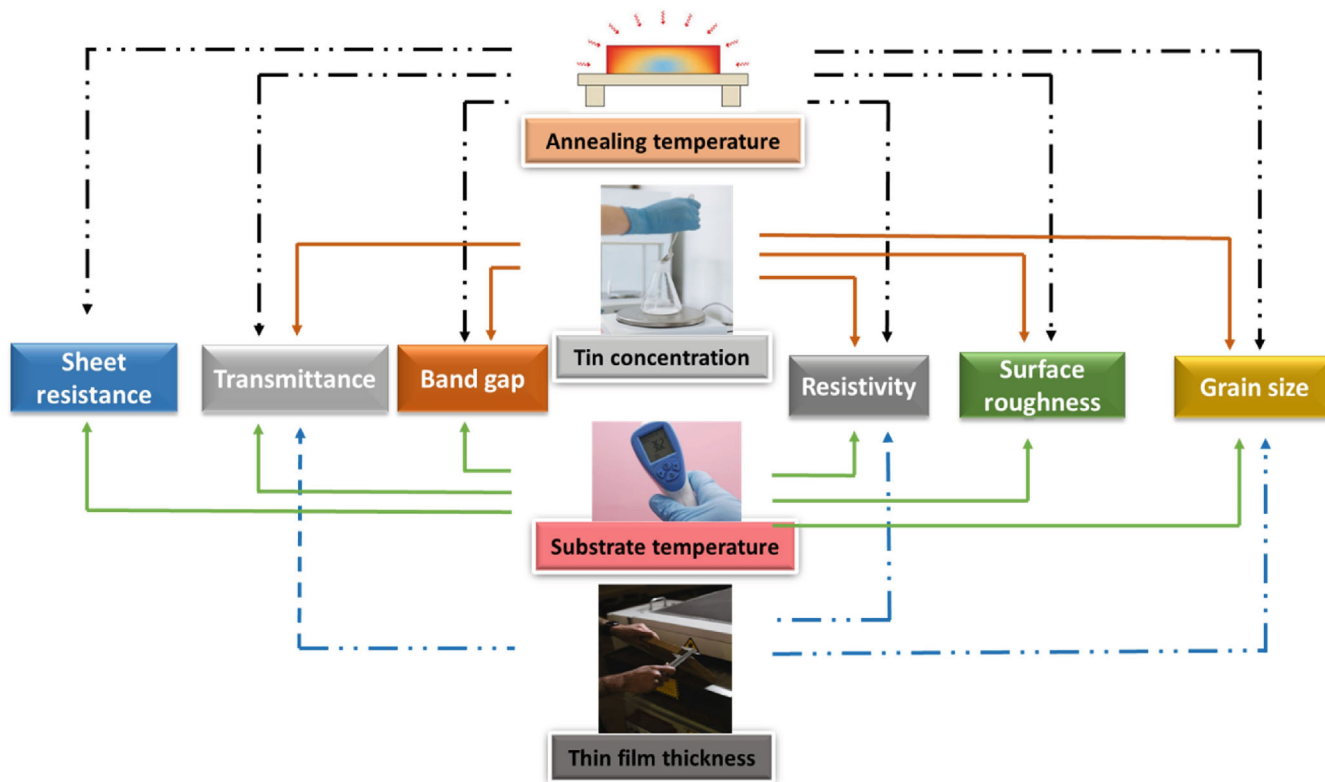
FIGURE 3 ITO thin films parameters relationship with annealing and substrate temperature, tin concentration, and ITO thin films thickness (authors original images, attribution is not required to part of the figures).

of annealing, the carrier concentration increased four times, and carrier mobility doubled compared to the as deposited thin film shown in Figure 4A. After the annealing process, the carrier concentration was 4.8×10^{20} cm^{-3} carrier mobility was 20 cm^2 V^{-1} s^{-1}. The thin film resistivity was minimized to 5.7×10^{-4} from 6×10^{-3} Ω cm with improved the crystallization. Alam and Cameron[1] investigated the relationship of between annealing temperature and resistivity ITO (10 wt.% Sn-doped) thin film prepared by the sol–gel dipping process. In this example, the annealing temperature ranged from 300°C to 700°C, with samples being annealed at each temperature (300°C, 400°C, 500°C, 600°C, and 700°C) for 1 h. Analysis showed that the electrical resistivity of ITO thin film decreased with increasing annealing temperature from 300°C to 600°C (Figure 4B). The resistivity of thin film calculated by using $\rho = \frac{(2\pi m * kT)^{\frac{1}{2}}}{De^2 n. \exp\left(\frac{-eV_B}{kT}\right)}$.[91] Additionally, the optical properties of the thin films were enhanced with annealing temperature. The transmittance improved from 80% for 400°C annealing to 93% for 600°C annealing, as shown in Figure 4C. The high-temperature (at 700°C) annealing guided thin films' steeper observation curve and showed excellent crystallinity and small defect density close to the band edge. The XRD spectrum (Philips X'pert XRD system, Cu target) analyses showed polycrystalline with a cubic bixbyite structure with no phases corresponding to the tin. Here, the tin was fully doped with In$_2$O$_3$ at an annealing temperature of 600°C. The SEM images of crystalline structure formation showed a clear improvement from as deposited to annealed thin film, as shown in Figure 4D,E. Beaurain et al.[92] investigated the effect of annealing temperature on the electrical properties of ITO thin films made through spin coating. The findings showed that as the annealing temperature increases, the resistivity of the ITO thin film decreases. The ITO crystalline morphology was found to be different after annealing, with the grain size increasing at 550°C compared to 350°C. Indeed, smaller crystalline sizes result in higher resistivity. However, the high-temperature annealing process is not applicable for ITO deposited on polymer (plastic) or textile substrates. Some applications require low-temperature annealed ITO thin films, especially when polymer or textile substrates need to remain flexible and have certain advantages.

Cho and Yun[26] deposited ITO thin film on a glass substrate by a sol–gel spin coating method. The ITO thin film was fired at 450°C–600°C for 30 min in air, followed by cooled down and then annealed at 450°C–600°C for 30 min under Ar (argon) atmosphere. The firing temperature of 500°C made the oxygen vacancies (creating free electrons) in the thin
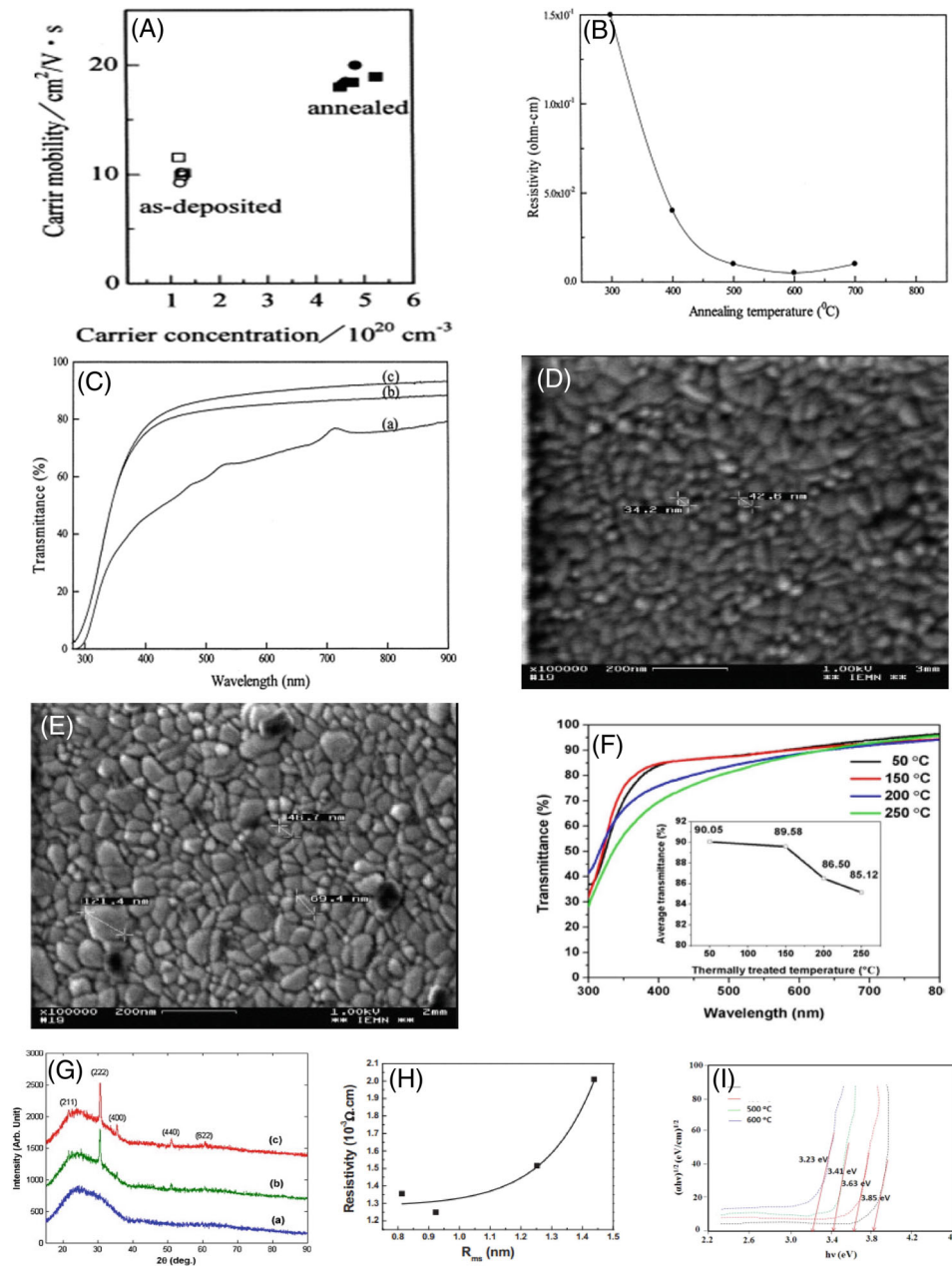
FIGURE 4 (A) Carrier concentration and carrier mobility relationship with annealing temperature (reproduced with permission),[3] (B) resistivity changes based on the annealing temperature of the ITO thin film (reproduced with permission),[1] (C) transmittance with the annealing temperature (a) 400°C, (b) 500°C, (c) 600°C (reproduced with permission),[1] (D) SEM image of as-deposited ITO thin film, and (E) annealed at 400°C (reproduced with permission),[89] (F) transmittance of the ITO thin films thermally treated (reproduced with permission),[27] (G) XRD pattern of the ITO thin films (a) as deposited, (b) 200°C, (c) 300°C for 1 h (reproduced with permission),[40] (H) relationship between surface roughness and resistivity (reproduced with permission),[90] and (I) electrical bandgap with the annealing temperature reproduced with permission.[31]

film. The thin film subsequently annealed at 500°C showed a lower sheet resistance (resistance of thin sheet multiplied by thickness) close to 361 Ω/area (author Cho and Yun[26] did not specify the area unit) with a grain size of 20–30 nm. However, the resistance increased above 500°C annealing due to microcracks on the thin film, which was observed by the field emissive – scanning electron microscope (FE-SEM, JSM-6430F.JEOL, Japan) at higher (600°C) annealing temperatures.

Dong et al.[27] synthesized an ITO thin film on the glass substrate by spin coating method with oxalic acid as a stabilizer and methylcellulose as a binder to enhance the conductivity and transmittance. The thin film was thermally heated

at 50°C, 150°C, 200°C, and 250°C before the final annealing at 500°C for 30 min with a heating rate of 5°C min^{-1}. Subsequently, the thin film was annealed in Ar/H$_2$ to decrease the resistivity further. The thermal treatment at 50°C removed moisture from the thin film, and temperatures above 150°C resulted in a small amount of crystallization, with a resulting thickness of 115 nm. Thermal treatment at 250°C increased the thickness to 180 nm. The increase in grain size led to a longer electron path, reducing grain boundary scattering. Consequently, this thin film exhibited increased conductivity and low resistivity (4.14×10^{-3} Ω cm). Note: analytically, the crystalline sizes can be calculated using the equation ($d = \frac{K\lambda}{\beta \cos\theta}$), where d is the mean crystalline size, K is the shape factor 0.89, λ is the wavelength of the incident beam, β is the full width at half maximum, and θ is the Bragg's angle.

Analysis showed that the resistivity decreased from 8.39×10^{-3} Ω cm to 4.14×10^{-3} Ω cm, and mobility increased from 7.59 to 14.80 cm^2 V^{-1} s^{-1} concerning the thermal treatment from 50°C to 250°C. A carrier concentration increase led to a bandgap of 3.75 eV at 150°C. The transmittance of ITO thin film decreased with increasing thermal treatment temperature from 50°C to 250°C due to a higher number of pores in the low-temperature level. The pores acted as a channel light that directly passed through ITO thin film. A high-temperature treatment reduces pores and resists light transmission, as shown in Figure 4F.

Daza et al.[16] deposited ITO (10 wt.% Sn, 99.99% purity from Cathay Advance Materials Limited, China) thin film on the glass substrate through RF sputtering at different inclination angle ($\alpha = 0°$, 40°, 60° and, 80°) and annealed samples at 250°C in air for 1 h. The high temperature was avoided to prevent the crystallization of negative optical effects on red and infrared regions. The XRD pattern showed that the most intense peak of In$_2$O$_3$ (222) was with other small peaks of $\alpha = 0°$ and 40° after annealing. Angle 80° samples showed surface defects due to the increased strain (ε) effect. The bandgap increased to 3.927 eV from 3.748 eV after annealing, and it was calculated using the equation $Eg = h\frac{c}{\lambda}$.[93] The porosity of thin film increased with the inclination angle due to fissures in the films, and the refractive index decreased from 2.1 to 1.95.

Raoufi et al.[41] deposited ITO (10 wt.% Sn, 99.99% purity from Merck Co) thin film on a glass substrate (temperature of 25°C) by EB evaporation (base pressure of 1×10^{-6} mbar, voltage of 1–10 kV, EB current 10–12 mA). Samples were annealed in a thermal furnace in the air at 200°C and 300°C for 1 h. The XRD patterns of the as deposited and different annealing temperatures are shown in Figure 4G. No diffraction peaks appeared on the deposited (non-annealed) ITO thin film. The peaks started to appear with the annealing temperature increased. The diffraction peaks (222) on the annealed (300°C) thin films confirmed the formation of the polycrystalline ITO thin films. The annealing process aggregated native grains into larger clusters. The larger clusters influenced and increased the surface height roughness (R_a) and the standard deviation of surface height values (RMS or root mean square roughness) as the annealing temperature increases. Raoufi et al.[40] also demonstrated and confirmed the surface roughness and RMS linear behavior with respect to the annealing temperature. The resistivity was found to be directly related to the surface roughness (Figure 4H). As a result of that, resistivity increased with higher annealing temperature due to the increased surface roughness. High surface roughness increased the possibility of electron scattering and reduced the accessible path for electrons.[90] Measuring the surface roughness of ITO thin films through SEM techniques is challenging. The UV–vis–NIR spectra technique and a calculation were developed to determine surface roughness using the formula $\delta = \frac{\lambda}{4\pi \cos\theta_0} (TIS)^{\frac{1}{2}}$, where δ – surface roughness, λ – wavelength, θ_0 – angle of incidence, TIS – total integrated scattering.[94]

Premkumar and Vadivel[31] deposited ITO (20 wt.% Sn, Sigma Alrich) thin film on the glass substrate by a spin coating method and annealed it at 300°C, 400°C, 500°C, and 600°C for 2 h. SnO$_2$ peaks were detected at lower annealing temperatures, and Sn was not fully doped with the In$_2$O$_3$. However, at higher annealing (600°C) temperature, no SnO$_2$ peaks were evidenced, which confirmed that Sn atoms were fully doped on the In$_2$O$_3$. The peak intensity also increased, confirming that the annealing process improved thin films' crystallinity. The average crystalline size increased with annealing temperatures of 300°C, 400°C, 500°C, and 600°C (25, 34, 46, and 55 nm), respectively. The electrical bandgap decreased from 3.85 to 3.23 eV with the change in annealing temperature, as shown in Figure 4I. However, a high temperature (above 600°C) of the annealing process led to microcracks and negatively affected the thin film performance. Previous studies on annealing temperatures below 700°C have also reported similar findings. Recently, Li et al.[45] conducted a study on the conductive stability of ITO thin film fabricated by the PLD deposition technique using high-temperature annealing (above 1000°C). The study observed minimal level of changes in conductivity, grain size, and crystallization of ITO thin film. Furthermore, increasing the annealing process time at 1000°C did not significantly influence the thin film properties. Based on these results, the low temperature is more appropriate to enhance the properties compared to 1000°C. The resistivity and surface roughness decrease, the polycrystalline structure forms, bandgap decreases, and transmittance increases through annealing at lower temperatures.

3.2 | Substrate temperature

The substrate temperature during deposition is one of the essential factors influencing ITO thin film performance. El Akkad et al.[17] and Nisha et al.[22] suggested that the thin film's electrical conductivity depends on substrate temperature and film composition. The substrate temperature plays a significant role in the crystallization of thin film during deposition and enhances their properties. The polycrystalline structure formation reduces the thin film resistivity and surface roughness. The high substrate temperature deposition process is like the annealing process. However, it is important to note that it is challenging to maintain the constant substrate temperature.

George and Menon[39] deposited ITO (20 wt.% Sn, 99.99% purity) thin film on a glass substrate by EB evaporation (vacuum pressure of 5×10^{-5} mbar, voltage of 6 kV, EB current 10–15 mA) and investigated the relationship between substrate temperature (50°C–350°C) and ITO thin film properties. Analysis indicates that the thin film's resistivity decreased with increasing substrate temperature due to the improved crystalline nature of thin film, shown in Figure 5A. Also, the lowest resistivity of 3×10^{-6} Ωm and a bandgap of 3.41 eV were obtained at a substrate temperature of 350°C.

Craciun et al.[44] utilized the UV-PLD method to develop the ITO thin films. They aimed to develop high-quality ITO (10 wt.% Sn, 99.99% purity) thin films using the UV-PLD approach with substrate temperatures range from 40°C to 180°C. The thin film showed an amorphous structure up to a substrate temperature of 70°C with high carrier mobility. Good crystallization was observed at 120°C along with the increased resistivity and decreased carrier mobility due to the crystallization, resulting in the formation of a defective layer in the structure.

Marikkannu et al.[58] deposited ITO (5 wt.% Sn) thin film on the glass substrate by jet nebulizer spray (JNS) pyrolysis with three different substrate temperatures (350°C, 400°C, and 450°C). As a result of substrate temperatures, a fine crystallization development confirmed by the presence of peaks (222) (400) in the XRD patterns, shown in Figure 5B. The SEM images of different substrate temperatures (Figure 5C–F), also confirmed effect of substrate temperature on crystallization. As a part of this study, transmittance was investigated in relations with the substrate temperatures. Thin film transmittance was studied by UV – Vis optical transmittance spectra from 300 to 800 nm wavelength range. The transmittance (60%, 70%, and 80%) of thin film increased with ITO thin film prepared temperature increases (350°C, 400°C, and 450°C) due to crystallization (Figure 5G). Sun, Wang and Kwok[23] deposited single ITO (10 wt.% Sn, 99.99% purity) thin film on a glass substrate and applied ZnO buffer before the ITO thin film using RF sputtering (Denton Vacuum, Inc model DVI SJ/24LL) with substrate temperatures ranging from 50°C to 300°C. Figure 5H illustrates the resistivity relationship with substrate temperature. Both the ITO-coated samples' resistivity decreased with increasing temperature. Especially the ZnO buffer on the glass substrate with ITO showed significantly lower resistivity due to an increase in oxygen ratio, reducing the electron scattering with concerning same substrate temperature conditions.

Jun et al.[21] initiated an investigation to determine deposition conditions for achieving high transmittance and low sheet resistance. ITO (10 wt.% Sn) thin film (300 nm) was deposited on a glass substrate using RF sputtering (AJA ATC2000) with a substrate temperature range from 30°C to 230°C. The analysis showed that the layer resistance decreased significantly with higher temperature deposition. The lower sheet resistance of 28 Ω m^{-1} was obtained at a substrate temperature of 230°C, RF power of 125 W, and pressure of 2 Pa. However, the transmittance decreased compared to other RF power (75 and 100 W) deposition conditions due to the low oxygen vacancies concentration formed. Increasing temperature enhanced the transformation of the ITO thin film from an amorphous to a crystalline structure. Higher RF sputtering power levels also enhanced the crystallinity of ITO thin film, as high power quickly melted particles and resulted in a higher degree of crystallinity.

Nisha et al.[22] deposited ITO (5 wt.% Sn, 99.99% purity) thin film on a glass substrate by RF sputtering with a substrate temperature range from room temperature to 250°C. Initially, XRD analysis confirmed the linear relationship between the intensity of peaks (222) (400) and substrate temperature, indicating crystallization. As a result, the resistivity of ITO thin film decreased with an increasing substrate temperature, shown in Figure 5I. The resistivity and sheet resistance decreased with an increase in substrate temperature up to 150°C. The grain size increased with deposition temperature, reducing grain boundary scattering, and increasing conductivity. Carrier mobility and carrier density increased with substrate temperature, leading to a significant decrease in resistivity, particularly around 150°C, due to better crystallinity of the thin film. The increase in resistivity observed above 200°C might be attributed to alkali ions contamination on the glass substrate. Transmission also increased with substrate temperature. High substrate temperature (250°C) showed an average above 80% transmission in the visual spectrum region. Substrate temperature also influenced the bandgap, which increased from 3.68 to 3.84 eV with the increase in substrate temperature.

Hoshi et al.[62] investigated the sputtering deposition rate relationship with the ITO thin film on glass, acryl, and polycarbonate substrate in low substrate temperature (below 80°C). As results showed that on a polycarbonate film substrate,
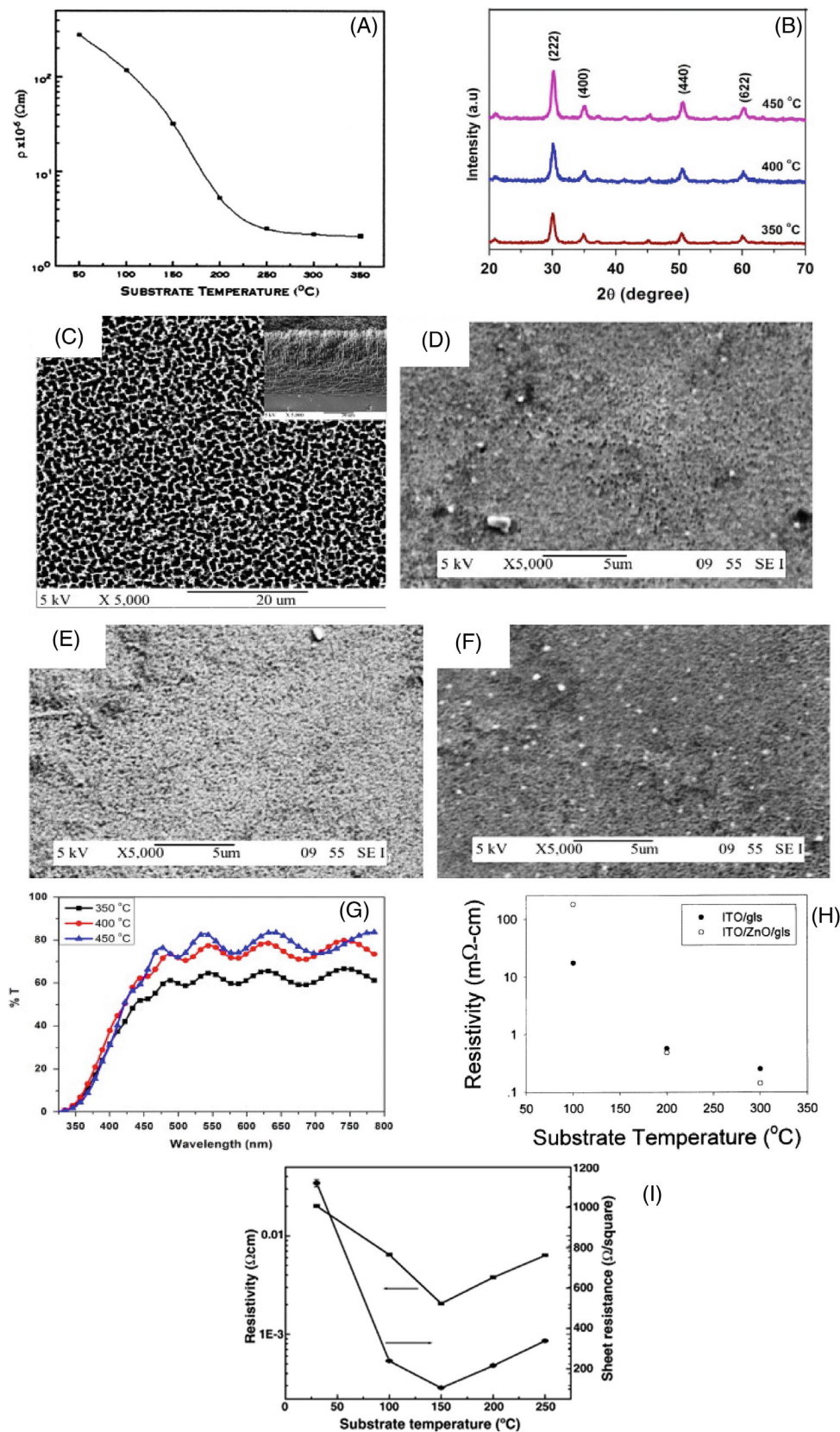
FIGURE 5 (A) Resistivity vs substrate temperature (reproduced with permission),[39] (B) XRD patterns based on substrate temperature (reproduced with permission),[58] SEM images of ITO thin films: (C) silicon substrate, ITO deposited temperatures (D) 350°C, (E) 400°C, and (F) 450°C (reproduced with permission),[58] (G) transmittance of the ITO thin films with different temperature preparation (reproduced with permission),[58] (H) films resistivity based on the substrate temperature (reproduced with permission),[23] and (I) resistivity and sheet resistance based on the substrate temperature (reproduced with permission).[22]

the deposition rates up to 53 nm min^{-1} thin films showed the lowest resistivity, with crystal growth promoted by a high oxygen flow rate. However, above 80 nm min^{-1} deposition rate, the thermal damage obtained on polycarbonate substrate by sputtering film fabrication. A facing target sputtering (FTS) system effectively deposit a rate of 100 nm min^{-1} thin films on an acryl substrate without thermal damage. Maintaining an appropriate substrate temperature helps in crystallization, grain size increase, and resistivity decrease of thin film. However, it is not always viable to maintain the substrate temperature in all types of thin film preparation, and in some cases, it requires special arrangements to keep the substrate temperature constant.

3.3 | Tin concentration

The concentrations of tin and indium chloride are critical factors in deciding ITO thin film properties. The optical properties and crystallization of ITO thin films strongly depend on Sn-doped concentrations.[42] The XRD results confirmed that doped films have larger crystalline size than non-doped ones. The electrical resistivity also depends on the atomic ratio of Sn:In of thin film.[47]

Nishio, Sei and Tsuchiya[80] investigated the thin film's electrical resistivity, carrier concentration, and mobility in the SnO$_2$ range of 0 mol% to 20 mol% with heat treatment from 400°C to 800°C for 1 h. In this study, a dip coating process was used to deposit the ITO thin film on a glass substrate. They observed low electrical resistivity of 1.2×10^{-3} Ω cm, a high carrier concentration of 1.2×10^{20} cm^{-3}, and more downward carrier mobility of 7.0 cm^2 V^{-1} s^{-1} at 12 mol% SnO$_2$. It was concluded that the crystallization of thin film started at a heat treatment temperature of 400°C and was fully crystallized at 600°C.

George and Menon[39] deposited ITO thin film on a glass substrate by EB evaporation with a tin oxide concentration level ranging from 10% to 80%. As a result, the thin film's resistivity increased with the percentage of tin oxide above 20%. The 20% and 40% concentrations of tin oxide resistivity increased from 7.6×10^{-3} Ωm to 1.92×10^{-2} Ωm. Further increase of tin oxide has not shown high resistivity changes, as shown in Figure 6A. Analysis showed that the initial resistivity decreased due to the gradual incorporation of tin impurity as dopants into the indium lattice. Also, the resistivity increased above 20% of tin concentration because of a higher concentration of tin than the optimum level, resulting in more tin ions settling in neighboring sites, which led to crystalline disorder.[1]

Senthilkumar et al.[42] deposited ITO thin film on a glass substrate by EB evaporation (base pressure of 5×10^{-5} mbar, voltage of 1–10 kV) with tin concentrations ranging from 0% to 20% to determine the optimal parameters for ITO thin film fabrication. The analysis suggests that the thin film grain size decreased with increasing tin concentration, as shown in Figure 6B. XRD results confirmed that ITO thin film had a partially crystalline nature, which was the reason for weak intensity peaks with tin concentration increases. Transmittance showed high level at zero tin (Sn) concentration, and the increase in Sn concentration led to an increase in oxygen vacancies and more grain boundaries. The scattering of light at the grain boundaries was the cause of the decrease in transmittance. An energy bandgap was 3.61 eV at zero tin concentration and increased to 3.89 eV at 20 wt.% of tin concentration. Alam and Cameron[1] deposited ITO thin film on a glass substrate by sol–gel dipping process with a tin concentration ranging from 0% to 20% and investigated the wt.% of Sn with electrical resistivity at an annealing temperature of 600°C. They concluded with 10 wt.% Sn-doped thin film showed lower resistivity of 1.5×10^{-3} Ω cm (Figure 6C).

The concentration level of indium chloride (InCl$_3$) can also influence ITO thin film properties. Moholkar et al.[59] investigated the effect of indium chloride concentration on the properties of ITO thin film by preparing ITO thin film using the spray pyrolysis method with increasing concentration level of InCl$_3$ from 6.25 to 37.5 mM. The thin film thickness increased with an increasing concentration level of InCl$_3$ from 6.25 to 25.0 mM spraying solution, shown in Figure 6D. However, the thickness decreased after 25 mM due to available oxygen from the H$_2$O molecule was insufficient to increase growth further. Additionally, the resistance decreased with increasing InCl$_3$ concentration. The low electrical resistance of thin film achieved in the deposition of InCl$_3$ 25 mM concentration at substrate temperature 500°C is shown in Figure 6E. Atomic force microscopy (AFM) imaging confirmed surface roughness and grain sizes were 35 nm and around 200 nm, respectively, for a thin film with InCl$_3$ 25 mM concentration. The tin concentration on the thin film is important to decide the performance of the thin film without annealing and other processes. An appropriate tin concentration results in the low resistivity, grain size, and Sn-doped crystalline structure. However, a high concentration of tin increases the resistivity of a thin film. Therefore, the right amount of tin concentration enhances the performance of the thin film, which can be further improved through the annealing process.
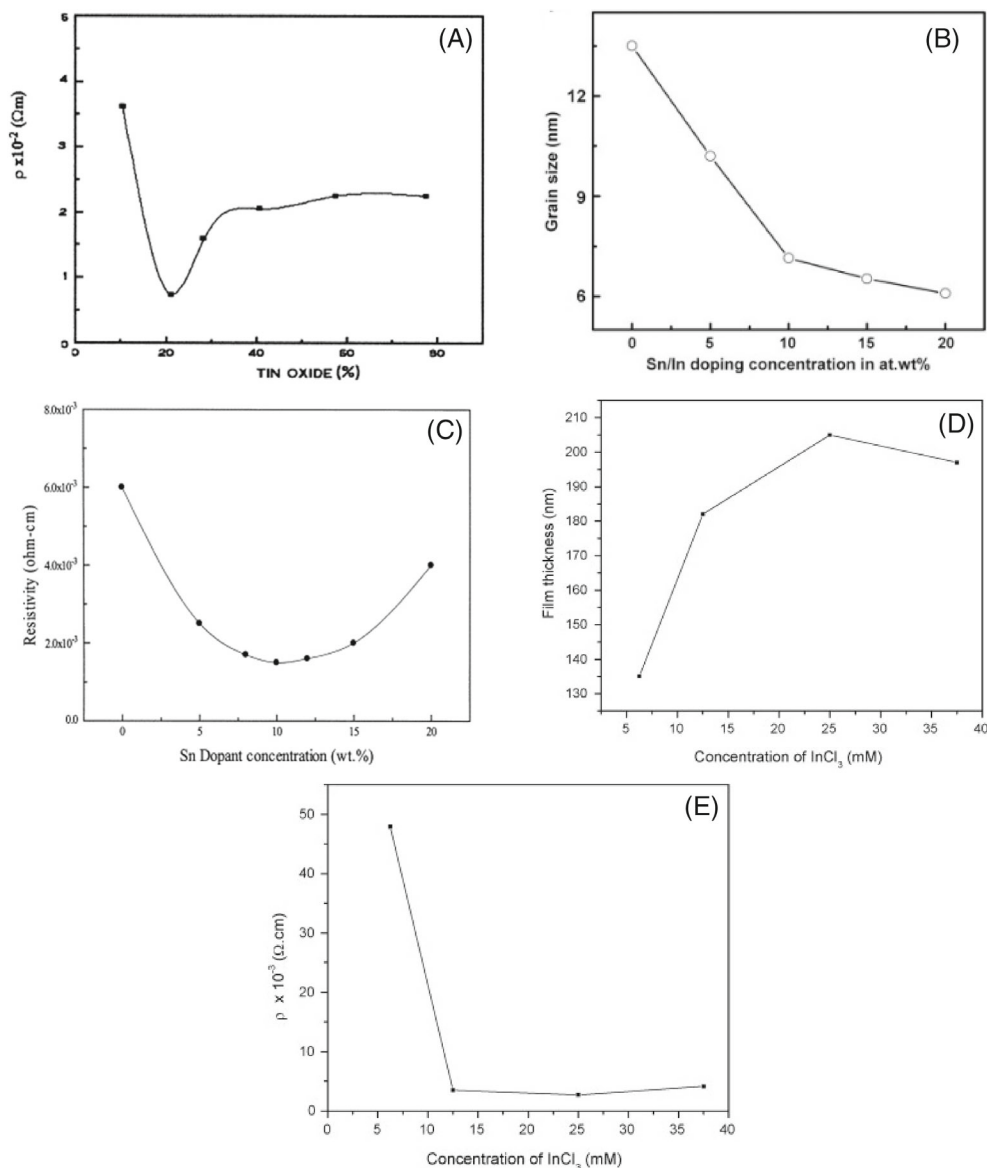
FIGURE 6 (A) Resistivity vs tin oxide concentration (reproduced with permission),[39] (B) variation of the grain size with respect to the Sn-doped concentrations (reproduced with permission),[42] (C) resistivity changes based on the Sn wt % at annealing temperature of 600°C (reproduced with permission),[1] (D) The thin film thickness increases with the concentration of the $InCl_3$ (reproduced with permission),[59] and (E) the electrical resistivity changes based on the concentration of $InCl_3$ (reproduced with permission).[59]

3.4 | Thin film thickness

The thickness of ITO thin film is crucial for thin film's resistivity, crystallization, and overall performance. The thickness significantly impacts structural, optical, and electrical properties. A high thickness of the thin film can be made through a high deposition rate in a short time. However, a high deposition rate can affect thin film behavior and the base substrate. Alternatively, a high thickness can be obtained through repeated coating and a low deposition rate for a long time. Gradual growth of thickness reduced resistance significantly. Other parameters of ITO thin film grain size, roughness, relative density, and pore size were influenced by thickness increases.[11]

Kumar, Raju and Subrahmanyam[11] deposited ITO (10 wt.% Sn, 99.99% purity) thin film on a glass substrate by DC magnetron sputtering (ANELVA model SPC-530H) at room temperature. Structural, optical, and electrical properties relationship with thin film thickness was examined through increasing the thickness from 165 to 1175 nm. The crystalline structure was studied using XRD (Philips X'pert Pro), and the diffraction peaks were observed for thicknesses above

380 nm (Figure 7A). The high thickness (1175 nm) showed various peaks indicating crystalline formation. The grain size and RMS roughness increased with thickness, which was attributed to decreases in transmittance. A low resistivity of 4.5×10^{-4} Ω cm, a high carrier concentration of 5.3×10^{20} cm^3, and low mobility of 26 cm^2 V^{-1} appeared on 545 nm thin film thickness.

Ghorannevis, Akbarnejad and Ghoranneviss[18] studied the physical properties of ITO thin films depending on the deposition time during radio frequency magnetron sputtering. The deposition time increased the thin film thickness from 100 to 300 nm and decreased crystal size from 25.440 to 17.226 nm. The SEM and cross-section thickness measurement images are shown in Figure 7B,C. The XRD pattern suggested that diffraction peaks increased with thickness increase, indicating crystalline formation. Surface morphology investigation by AFM showed that grain size and surface roughness (3.93–5.18 nm) increased with thickness from 100 to 300 nm. Increasing the film thickness from 100 to 300 nm reduced resistivity from 15.4×10^{-4} Ω cm to 2.43×10^{-5} Ω cm. At a thickness of 300 nm, lower resistivity was observed due to improved crystallinity, high oxygen vacancy concentration, and grain growth, which decreased grain boundary electron scattering. Increasing thin film thickness reduces resistivity and transmittance while increasing grain size and carrier concentration. However, high thin film thickness increases the resistivity and negatively influences properties. An appropriate thin film thickness enhances the thin film performance, and annealing can further improve the thin film.

Davood and Faegh[38] investigated the surface morphology changes on ITO (10 wt.% Sn) thin film on the glass substrate with different thicknesses (ranging from 100 to 350 nm) using the EB deposition method. The AFM study revealed the formation of a porous granular surface as a surface roughness linearly decreased from 24.8 to 4.13 nm, with thickness increasing from 100 to 350 nm. Teixeira et al.[14] studied ITO (10 wt.% Sn, 99.99% purity) thin film deposited on a glass substrate by DC magnetron sputtering with film thickness ranging from 50 to 900 nm. The resistivity of ITO thin film increased with increasing thickness, as shown in Figure 7D. The lower resistivity of 2.35×10^{-4} Ω cm was observed with a film thickness of 282 nm due to the physical properties of a thin film being different from bulk material. Initially, the thickness increase reduced the resistivity up to a thickness of 282 nm. However, after that point, the resistivity increased due to the addition of multiple layers, which resulted in decreased carrier mobility and carrier concentration. The formation of voids increased charges carrier scattering, leading to an increase in resistivity with thickness.

Ota et al.[3] deposited ITO thin film on a glass substrate by dip coating process with repeated dipping of ten layers, followed by a heating process to dry each layer. A film thickness of 112 nm showed low resistivity of 5.8×10^{-4} Ω cm after 10-layer deposition. As previous studies suggested, a thin film thickness of approximately 300 nm showed minimum resistivity of 4×10^{-4} Ω cm. The resistivity of the thin film is influenced by the deposition method. Herrero and Guillen[20] deposited ITO thin film on a glass substrate by RF sputtering with a thickness range of 175 to 450 nm. The XRD results indicated an increase in the intensity of the (222) peak with increasing thickness, indicating crystallization (Figure 7E). The resistivity decreased from 4.0×10^{-3} Ω cm to 1.2×10^{-2} Ω cm, and the transmittance increased from 87% to 91%, with thickness increasing from 175 to 450 nm, due to an improvement in grain size enhancing conductivity (Figure 7F).

Suitable annealing and substrate temperature, tin concentration, and thickness of the thin film makes ITO thin film with properties such as low resistivity, a polycrystalline structure, increased grain size, changes in band gaps and Sn fully doped in In$_2$O$_3$ and high transmittance. The low resistance of the ITO thin film obtained at the high grain size condition prevents electron scattering, enhancing the thin film's performance. Morphology changes from amorphous to polycrystalline structure provide a smooth surface roughness. Minimization of the bandgap improves the conductivity of the thin film.

Not all the literatures investigated the ITO thin film crystalline formation with Raman spectroscopy and X-ray photoelectron spectroscopy (XPS). However, few of them are summarized here. Lian et al.[96] deposited ITO thin film on a glass substrate using EB evaporation. The deposited substrates underwent annealing in the range of 150°C–450°C. Oxygen vacancy defect states and vibrational levels within the ITO thin films were investigated by Raman scattering. The results confirmed that oxygen vacancy defects have a significant influence on the vibration of the In–O–In bond, causing variations in Raman scattering intensity and shifts in Raman peak position. The reduction in Raman scattering intensity results from a decrease in oxygen vacancies after annealing. The results indicated that partial oxygen vacancies were filled during the annealing process, and the broken In–O–In bonds confirmed the dissociated and agglomerated rough surface. Hong et al.[97] deposited ITO thin film on a glass substrate using EB evaporation. Subsequently, laser irradiation treatments were performed on the surface of the ITO thin film. Raman spectroscopy was used to study the effects of laser intensities on defect formation and vibrational modes of the ITO thin film. Following laser irradiation, the Raman scattering
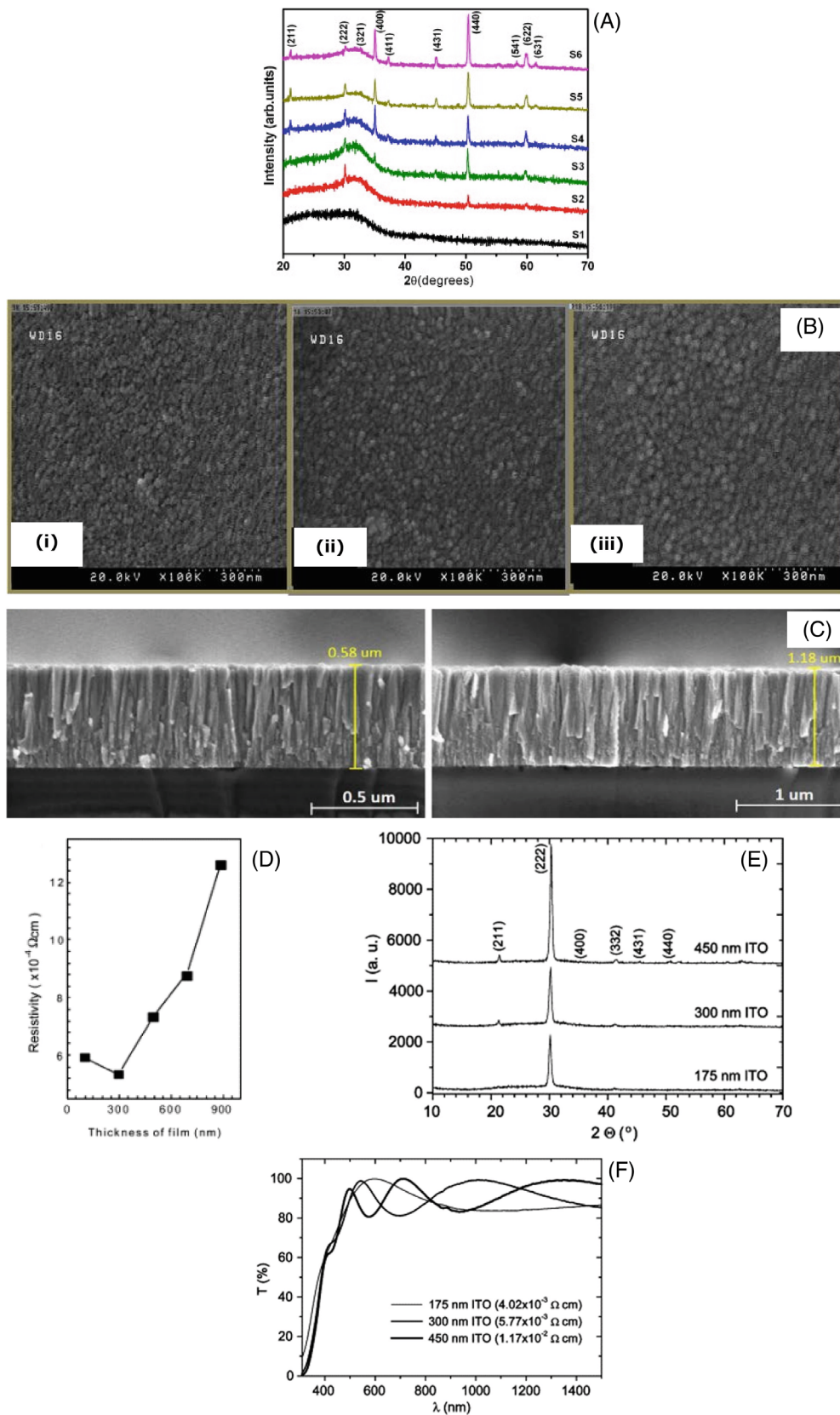
FIGURE 7 (A) X ray diffraction with different thickness (reproduced with permission),[11] (B) SEM image of ITO thin films based on thickness (i) 100 nm, (ii) 200 nm, (iii) 300 nm (reproduced under the terms of the Creative Commons Attribution 4.0),[18] (C) cross-section view of thickness (reproduced under the terms of the Creative Commons Attribution 3.0),[95] (D) the resistivity increases with the thickness (reproduced with permission),[14] (E) XRD results of different thickness films (reproduced with permission),[20] and (F) transmittance based on thin film thickness (reproduced with permission).[20]

intensities of all the irradiated ITO thin films were higher than those of the as-deposited thin films. The high scattering intensity resulted from the laser, which disrupted and recombined the internal structure of the ITO thin film, enhancing intergrain scattering. Additionally, the peak intensities decreased with further increases in laser power, leading to more defects. Another factor to consider is that the removal of ITO thin film thickness resulted in a new vibrational mode at 173 cm^{-1}.[97] Singh et al.[83] deposited ITO thin film on glass substrate by spin coating. Raman analysis of ITO thin film carried out to analyze the vibrational and transmittance features. The Raman results showed and confirmed that SnO_2 along with indium doped SnO_2 observed peaks at 472, 634 and 761 cm^{-1}.

Al-Kuhaili[98] deposited ITO thin film on the fused silica and molybdenum substrates using DC magnetron scattering at the substrate temperature of 350°C. XPS used on the molybdenum substrate to see the charging of the non-conducting samples could be reduced. The result peaks showed that, 3d core level of indium and tin consists of two sublevels of $3d_{3/2}$ and $3d_{5/2}$ due to spin orbit splitting. The first component binding energy (BE) of 529.8 ± 0.2 eV, indicates the In-O bond in In_2O_3 and the second component BE of 530.4 ± 0.2 eV, was assigned to the Sn−O bond in SnO_2. The third component BE of 531.2 ± 0.1 eV corresponds to the oxygen vacancies in O 1s spectrum. The XPS confirmed that the indium and tin atoms bonded to oxygen and presence of oxygen vacancies in thin films. Hsu et al.[99] prepared ITO thin films on a glass substrate using plasma-enhanced atomic layer deposition (PEALD). XPS results confirmed the successful incorporation of Sn into In_2O_3. Two distinct peaks were observed at 486.1 eV and 495.3 eV which corresponded to $Sn3d_{5/2}$ and $Sn3d_{3/2}$, respectively. The presence of Sn^{4+} and Sn^{2+} components led to further splitting of each peak. No metallic Sn component peak was observed. However, Sn^{2+} and neighboring Sn^{4+} did not contribute to the improvement of the conductivity of ITO thin films. To achieve higher conductivity and an improved free electron concentration, the peak ratio of Sn^{4+} needs to be increased as much as possible.

Overall, the annealing temperature has a very close relationship with the properties of ITO thin film, as it enhances crystallinity and increases grain size. As per various studies presented above, an annealing temperature of typically 600°C is very appropriate for excellent properties of the ITO thin film. It is important to note that high annealing temperature can induce microcracks (potentially due to thermal strain) in the thin film and increase resistance. The substrate temperature is also significant in deciding the performance of thin film. The crystallinity of thin film improves with an increase in substrate temperature. However, a substrate temperature (above the room temperature) is not applicable for all the preparation conditions due to the need for special arrangements to keep the temperature stable. A substrate temperature maximum of 200°C is suitable for getting a better property of thin film. Higher substrate temperature can result in alkali contamination on a glass substrate, increasing resistivity. The optical properties of ITO thin film are highly dependent on the tin concentration. Higher tin concentration level shows better doping of In and Sn. A maximum tin of 10% is suitable for thin film. Higher tin concentration can lead to crystalline disorder. Thickness has a very significant impact on thin film properties. Increasing thickness improves the grain size and crystallinity. The ideal thin film thickness is approximately 300 nm for ITO thin film preparation. Higher thickness deposition increases the resistance of the thin film.

4 | ITO THIN FILM FOR HUMIDITY SENSING APPLICATIONS

This section discusses the ITO thin film humidity sensing and its limitation.

In a recent review on humidity sensor, Kuzubasoglu[100] discussed that the conductivity of a thin film is influenced by the sensitive signals from water molecules in humidity-sensitive materials. Hydrogen bonds, intramolecular contacts, electrostatic interactions, hydrophilic and hydrophobic interactions, chemical bonding, etc, are some types of these interactions. To describe the process of humidity sensing, two different humidity sensing mechanisms (chemisorption, physisorption) are significant. The chemisorption mechanism is significant at low relative humidity (or high temperatures), and physisorption plays a key role at high relative humidity (or low temperatures). Chemisorption relates to the chemical reaction between water molecules and the material, while physisorption is more related to the physical absorption of water molecules by van der Waals forces. In a wide range of applications, combined sensing mechanisms take place.[101] Figure 8A,B illustrates the mechanism of ITO thin film interaction with H_2O molecules in the context of humidity sensing. The sensitivity of ITO to humidity primarily depends on the low and high reactive humidity levels. In lower relative humidity level (about 10%–30%), H_2O (water) molecules absorb on ITO thin film and applied DC voltage ionizes water molecules into H^+ and OH^-. In the higher relative humidity range (about 50%–90%), a multilayer of H_2O molecules produces hydronium groups (H_3O) and OH^- as electron donors, leading to a decrease in thin film resistance and an increase in electronic mobility and conductivity as well.[31] The schematic diagram (Figure 8C) presents the measurement of resistance/capacitance changes based on the humidity level on the ITO thin film.
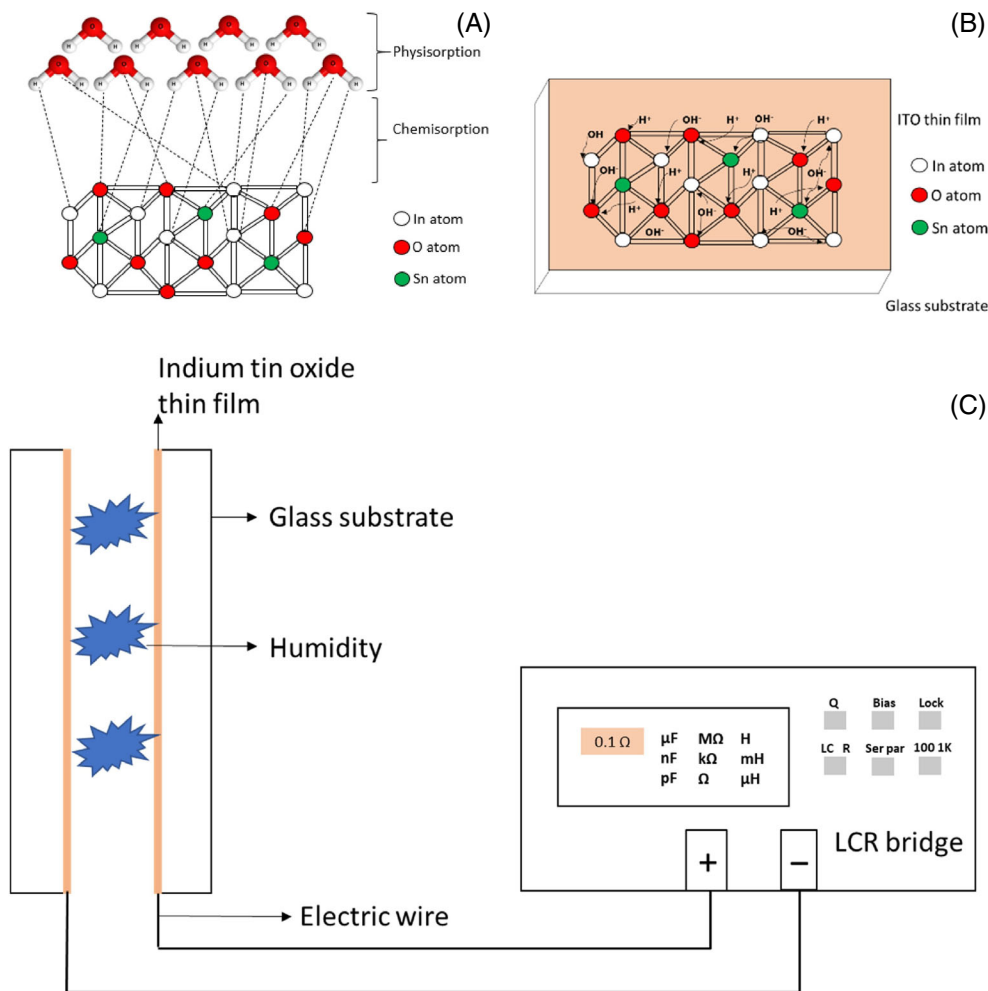
FIGURE 8 (A) Water molecules absorption on ITO, (B) water molecules interaction with ITO thin film, and (C) capacitance/resistance measurement based on humidity (authors original image).

Table 1 presents different ITO thin film humidity measurement approaches based on resistance and capacitance changes. It has been demonstrated that capacitance increases with the presence of relative humidity range increase. Based on the previous studies, the resistance of ITO thin film decreased with an increase in relative humidity ranging from 5% to 98% at room temperature due to the many electrons released from water molecules. Premkumar and Vadivel[31] investigated ITO thin film humidity sensing behavior based on thin films annealed at different temperatures. Figure 9A shows that the resistance decreases (for different temperature annealed films) with relative humidity ranging from 10% to 90%. The higher temperature annealed thin film showed larger resistance drops due to improved crystallite and smaller energy bandgap. The sensitivity of ITO thin films is shown in Figure 9B. Analysis showed that the sensitivity range increased with an increase in relative humidity for all thin films. However, the thin film annealed at higher temperatures demonstrated higher sensitivity and greater stability compared to one annealed at low temperatures.

The response and recovery times are significant for evaluating humidity sensing efficiency of thin film. Premkumar and Vadivel[31] demonstrated humidity thin film performance of low temperature (i.e., 300°C) annealed thin film had an average response and recovery time of 68 and 54 s, respectively. The response and recovery time were enhanced at higher temperature (600°C), annealing 28 and 14 s. High-temperature annealed thin film showed high sensitivity, quick response, and recovery time compared with other annealed thin film shown in Figure 9C. Babu and Vadivel[25] showed sensitivity, response, and recovery time behavior of thin film as prepared (without annealing) and after annealing (at 500°C). Resistance decreased from 65 to 15 MΩ with an increased relative humidity of annealed thin film. As prepared, ITO thin film showed that resistance decrease from 90 to 45 MΩ with an increase in relative humidity. The humidity sensitivity performance of annealed ITO thin film increased with an increase in relative humidity. The response and

TABLE 1 Overview of ITO thin film humidity sensing measurement.

Sr. no	Materials	Measuring parameter	Type	Measuring instrument	References	Remarks
1	ITO and aluminum oxide ink (as a layer applied)	Capacitance	Active	UNI-T digital LCR meter (UT612)	McGhee et al.,[50]; McGhee et al.,[54]	Traditional parallel two plates
2	ITO applied on glass plate	Resistance	Active	Keithley Electrometer	Yadav et al.,[34]	–
3	ITO applied on glass substrate	Resistance	Active	LCR bridge	Babu and Vadivel,[25]	Traditional parallel two plates
4	ITO thin film on glass substrate	Resistance	Active	LCR bridge	Premkumar and Vadivel,[31]	Traditional parallel two plates. Annealing temperature enhanced the sensitivity of ITO.

recovery time of annealed thin film enhanced compared to the as-prepared thin film, as shown in Figure 9D. Note, the sensitivity of ITO thin film can be evaluated with LCR bridge (used to measure the inductance (L), capacitance (C), and resistance (R) of components), and the humidity level can be measured through a standard hydrometer[31]: $S = \frac{RH_2 - RH_1}{RH_1} \times 100$, where S is sensitivity, RH_2 is resistivity measured in high relative humidity, and RH_1 is resistivity measured in low relative humidity. RH is also expressed on a scale of hundreds and is called a percentage relative humidity ($\%RH$): $\%RH = \frac{\text{Water vapour pressure}}{\text{Saturated water vapour pressure}} \times 100$.

Yadav et al.[34] reported nanocrystalline ITO thin film synthesis and humidity sensing response. ITO thin film was deposited on a glass substrate by the spin coating method with a synthesized $SnO_2 - In_2O_3$ nanocomposite. Followed by that, the thin film was dried at 120°C for 4 h and annealed at 500°C in the furnace to enhance their properties. The surface morphology of nanocomposite thin film studied revealed a nanostructured polycrystalline cluster with space of pores on the thin film's surface. Here, the XRD peaks were accordingly matched with the SnO_2 or In_2O_3 index. The small crystalline size of thin film enhanced thin film's humidity sensitivity. Transmission electron microscope (TEM) image of ITO thin film indicated grain's diameter ranged from 10 to 40 nm, and most grains were spherical. Figure 9G illustrates ITO thin film humidity response in three stages (I, II, and III). A rapid decrease in resistance value was observed in the low humidity range of 10% to 40% (stage I). In mid of humidity level (stage II), from 40% to 70% resistance range of decrease was small compared to stage I. In stage III, high humidity levels from 70% to 90% resistance decrease observed gradually. The sensitivity was found to be 1.20 MΩ/%RH, 0.61 MΩ/%RH, and 0.09 MΩ/%RH of ITO concerning the humidity level in three stages I, II, and III, respectively. The average sensitivity was 0.68 MΩ/%RH. The ITO thin film showed a high humidity sensitivity (1.20 MΩ/%RH) in low relative humidity concentration. In lower relative humidity, water molecules were absorbed on thin film dominant for electrical conduction. In high relative humidity, the amount of water molecules was high and provided a high number of electron donors, which reduced resistance at a high level. The water absorption enhanced electrical conductivity by increasing the electrical charge carriers and protons in the thin films' water absorption system. The electrical conductivity also depended on pores on the thin film surface. The resistance of thin film varied with RH measured using Keithley electrometer.

McGhee et al.[50] and McGhee et al.[54] tested the humidity sensing response of thin film designed by a screen-printed process. ITO and aluminum oxides (Al_2O_3) were utilized to make the metal oxide thin films through screen printing with two different surface area (4 and 9 cm²). ITO electrodes were printed and cured in a box oven at 105°C on polyethylene terephthalate (PET) substrates. The alumina dielectric ink was printed on top of dielectric film 1–6 times to eliminate the pinholes. In each print, the alumina dielectric ink was cured at 105°C, and the advantage of alumina was that it provided high capacitance. The final layer of ITO thin film and silver contacts were printed and cured at 105°C for 5 min. The UNI-T Digital LCR meter (UT612) was used to measure the capacitance (recorded in UNI-T digital multimeter software). Based on relative humidity increase (from 5 to 95 %RH), the capacitance value changed from 100 to 600 pF at four different frequencies 100 Hz, 1 kHz, 10 kHz, and 100 kHz. The surface area significantly impacted the thin films' response and recovery time. The smaller surface area (4 cm²) thin film showed a quick response time (21.4 s). The larger surface area (9 cm²) thin film showed response and recovery times of 47.2 and 49.5 s, respectively. The larger thin film surface took a
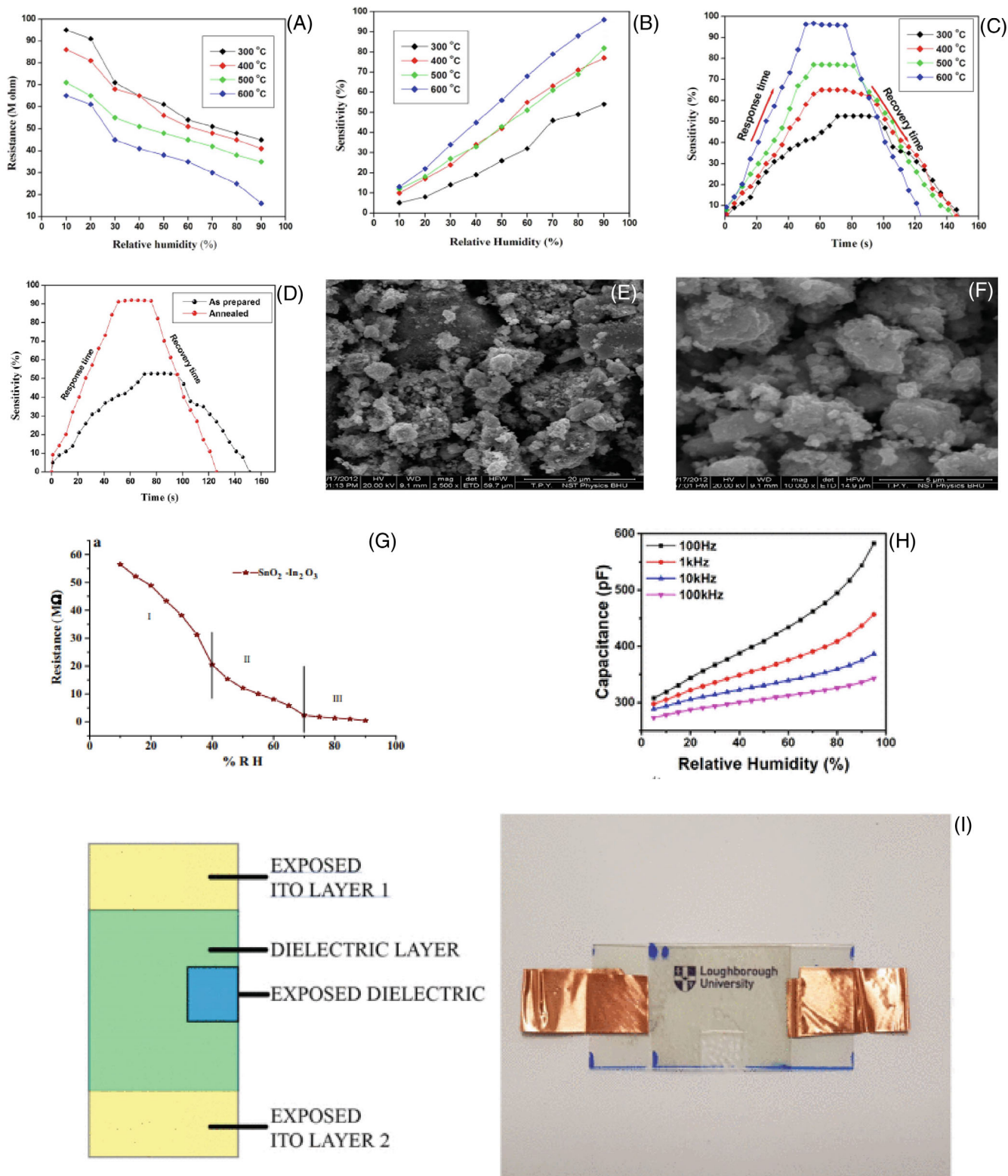
FIGURE 9 (A) Resistance changes on the ITO thin film based on relative humidity (reproduced with permission),[31] (B) ITO thin film sensitivity with relative humidity (reproduced with permission),[31] (C) sensitivity response with annealing temperature (reproduced with permission),[31] (D) the sensitivity of the two different thin film (reproduced with permission),[25] (E) SEM magnification of 20 μm (reproduced with permission),[34] (F) SEM magnification of 5 μm (reproduced with permission),[34] (G) ITO thin film humidity response (reproduced with permission),[34] (H) capacitance response based on the frequency measurement (reproduced under the terms of the Creative Commons CC-BY),[54] and (I) thin film with dielectric ink and copper tape (reproduced under the terms of the CC BY 4.0).[12]

long recovery time due to the dielectric layer requiring more time to reach a saturation level of water absorption, where diffusion was slow.

Table 2 presents various ITO thin films' response and recovery times. The response and recovery times are highly dependent on the preparation method, post processing and humidity level. Particularly, annealing ITO thin films supported quick response and recovery times. The capacitance increased with a rise in relative humidity in all four frequencies because water absorption changed the dielectric properties of alumina. The thin film measured relative humidity from 5% to 95% in a controlled environmental temperature of 25°C. The average thin film sensitivity was 3.8 pF/RH%, 2.11 pF/RH%, 1.185 pF/RH%, 0.85 pF/RH%, and the standard error mean of 0.42 pF/RH%, 0.23 pF/RH%, 0.12 pF/RH%, 0.092 pF/RH% with, respectively, to frequency measurement of 100 Hz, 1 kHz, 10 kHz, and 100 kHz. The thin film's sensitivity decreased with an increase in frequency due to the relative permittivity of the capacitor decreasing with increasing frequency, as shown in Figure 9H. Permittivity was the ability of the electrical storage of thin film, which decreased because the polarization of thin film increased in higher frequency. Analysis showed that the overall percentage of capacitance increased 204%, 164%, 140%, and 127% with 100 Hz, 1 kHz, 10 kHz, and 100 kHz, concerning relative humidity from 5% to 95%. The lower frequency measurement provided a higher response to humidity. Meanwhile, the thin film stability measurement was carried out with four different humidity operation conditions for two different thin film's surface areas. Analysis showed that the long-time humidity absorption on the layer did not damage the coating layer. In lower relative humidity, capacitance on both thin films decreased slightly over 7 days of the stability measurement period. In high relative humidity, capacitance gradually increased with days moving up to 45 days. It is important to note that thin film stability was high and did not show any damage in low and high relative humidity due to metal oxides being naturally highly stable.[12,54] The results of the experimental studies indicate that the presence of humidity does not affect stability of the ITO thin film. The stability of ITO thin film is considered one of the advantages in designing ITO-based humidity sensor.

T A B L E 2 Response and recovery time.

Sr. No	Coating material	Deposition	Response time	Recovery time	Sensitivity	Remarks	References
1	ITO/Alumina	Screen printed process	13.5–26.5 s	4–6 s	0.85–7.76 pF/RH%	Humidity ranges from 5% to 95% (surface area 4 cm²)	McGhee et al.[54]
2	ITO/Alumina	Screen printed process	47.2–56 s	49–76.5 s	0.85–7.76 pF/RH%	Humidity ranges from 5% to 95% (surface area 9 cm²)	McGhee et al.[54]
3	ITO	Sol–gel spin coating	75 s	65 s	Close to 50%	Relative humidity ranges from 10% to 90%	Babu and Vadivel,[25]
4	ITO	Sol–gel spin coating	58 s	45 s	Close to 90%	Relative humidity ranges from 10% to 90% (Annealed at 500°C)	Babu and Vadivel,[25]
5	ITO	Sol–gel spin coating	68 s	54 s	Close to 50%	Relative humidity ranges from 10% to 90%	Premkumar and Vadivel,[31]
6	ITO	Sol–gel spin coating	28 s	14 s	Close to 95%	Relative humidity ranges from 10 to 90% (Annealed at 600°C)	Premkumar and Vadivel,[31]
7	ITO/dielectric ink	Magnetron sputtering/screen printing	31.5 s	31 s	–	10 Ω/Sq sheet resistance, RH 5–95%	McGhee et al.[12,50]
8	PLA-TiO₂ on ITO plate	Spin coating technique	40 s	20 s	–	RH levels from 70% to 90%	Mallick et al.,[102]

McGhee et al.,[12] deposited ITO thin film on the PET substrate by magneton sputtering with sheet resistances of 10, 20, and 50 Ω/area (note: the author did not specify the area unit). By screen printing, dielectric ink (D2150901D1) was printed on the surface area of 7.5 cm^2 of 10 cm^2 of the ITO thin film. A 1 cm^2 surface area of wet dielectric removed and exposed dielectric while forming a parallel plate capacitor of ITO thin film. The thin film was cured with a UV lamp (365 nm) for 5 min. The copper tapes were placed on exposed ITO thin film on both sides to enhance electric contact, as shown in Figure 9I. The capacitance was measured through the UNI-T digital LCR meter (with UNI-T digital multi-meter software). The capacitance was measured at three different frequencies of 100 Hz, 1 kHz, and 100 kHz. Analysis showed that the capacitance increased with frequency in the relative humidity range of 5%–95% with all the frequencies, and capacitance behavior was linear with relative humidity above 75% due to water having a larger effect on the dielectric permittivity of thin film. Also, the lower sheet resistance (10 Ω/sq) showed a higher humidity sensitivity with the fixed relative range than the other two thin films. Noteworthy, the stability of thin films gradually changed with an increase in relative humidity (90%) because humidity trapped into the dielectric layer, which changed the dielectric constant and affected the thin film's stability. Also, this thin film was highly suitable for the measurement range of 5% RH to 75% RH.

Sajid et al.[103] reviewed the progress and future of humidity sensors from a materials perspective. To date, more than many research articles have been published on the development of humidity sensors. The summary includes a comparison of polymers, carbon-based materials, 2D materials, composites, and hybrid materials in relation to humidity sensing. Multidisciplinary and interdisciplinary research on humidity sensors is ongoing, addressing various parameters such as sensitivity, humidity range, response and recovery times, temperature dependence, and cost. Kuzubasoglu[100] provided a mini review of recent studies on humidity sensors. The study summarized a wide range of sensitive materials, including polymer-based, carbon-based, metal oxide-based, and composite-based sensors, and three different humidity sensing mechanisms were elaborated. The ideal specifications for humidity sensing materials included a high response to water vapor, low sensitivity to other gases in the atmosphere, a long operating life, cost-effective technology, high reproducibility, and a uniform and strong binding to the substrate's surface. Oh et al.[104] investigated the mechanical properties of freestanding ITO thin films in relation to annealing. In their investigation, the freestanding ITO thin film was prepared using various sub-steps. As-deposited thin films exhibited an amorphous structure and crystallized at an annealing temperature of 200°C. It was observed that the sheet resistance and transparency changed with the annealing treatment, especially since residual stress was eliminated when the ITO thin film was removed from the confining substrate. Further investigation showed that the young's modulus of the thin film increased with higher annealing temperatures. Analysis showed that the surface morphology was highly dependent on the annealing temperature, and the surface roughness of the ITO thin film decreased from 15.1 to 4.0 nm as the annealing temperature increased. Other mechanical properties such as elongation and tensile strength of the ITO thin film increased up to an annealing temperature of 150°C and then decreased at 200°C. Such behavior was attributed to excessive annealing temperatures leading to intrinsic material failure. Overall, the freestanding investigation method has the advantage of facilitating a better understanding of the intrinsic properties without being affected by residual stress.

Not only are ITO thin films used for humidity and other sensing applications, but ITO-coated substrates and ITO layers have also been employed to enhance the crystal quality and sensing abilities of layers.[105] The properties of advanced materials (i.e., nanomaterial) layers exhibit a strong relationship with the properties of the underlying ITO layer, including surface roughness, crystalline density, and morphology, which were investigated by Alsultany et al.[106] Saleem et al.[107] developed nanostructured multilayer MgF$_2$ on ITO-coated glass substrates at various substrate temperatures. The surface roughness of the coatings decreased as the substrate temperature increased, resulting in higher optical transmittance at lower substrate temperatures. Additionally, nanostructured multilayer MgF$_2$/ITO coatings at higher temperatures demonstrated higher shielding effectiveness in the decibel range, making them suitable for aerospace and defense applications. Recently, this study disclosed the enhancement of adhesion strength of ITO thin film by the inkjet printing method. Subsequently, the study investigated the impact of printing parameters on the adhesion strength of thin films. The inkjet procedure was performed at different nozzle speeds and with a different number of layers on a ceramic substrate. Based on the surface morphology results, the adhesion strength of a single layer is much lower than that of two layers and three-layer films due to the very thin and brittle layer being easily damaged under scratch loading. However, multilayers on the substrate increase the internal stress of the substrate, leading to cracks. Furthermore, in inkjet printing, the time gap between each layer and printing speed affects the strength of adhesion.[108]

5 | CONCLUDING REMARKS

This review summarizes the preparation of ITO thin films and explores property relationship with annealing temperature, substrate temperature, tin concentration, thin film thickness, and its ability to sense humidity. The acquired knowledge can be utilized for the development of advanced ITO thin films to monitor humidity levels at interfaces. Excessive humidity trapped in single and multilayer interface conditions can lead to significant structural failures. The challenge is inspecting the interface conditions frequently to ensure safe operations. Additionally, using large humidity sensors at interface is not viable, and monitoring conditions away from the interface does not provide real interface humidity conditions. The primary potential application of this ITO thin film preparation and future miniature sized sensor design is to effectively monitor interface conditions in various industrial applications. This review concludes with recommendations for improved ITO thin film preparation parameters to enhance its performance and properties, leading to an efficient sensor design. The selection of deposition method and base materials (e.g., glass, PET) are based on the applications of ITO thin film. Various thin film preparation methods make the ITO thin film for different applications with their own advantages and limitations. Literature shows that spin coating could be more advantageous for thin film preparation than other preparation methods due to its low fabrication cost, ease of preparing the solution, and ability to fabricate large and small thin films. Some properties are independent of the preparation method and synthesis protocols, while other depend on the compound concentration, thickness, and annealing process.

This critical review aims to provide a more suitable ITO thin film preparation method and preparation conditions for developing advanced, highly sensitive thin films for humidity measurement. Limitations and advantages associated with each parameter involved in ITO thin film preparation were discussed. The literature shows that the polymeric substrate could not withstand a high annealing and substrate temperature processes, which is the reason for typically using glass substrates. However, in lower operating temperatures and in certain applications, the polymer substrate could be used as a base material due to its flexibility and low-cost advantages. Also, it has been found that certain range of annealing and substrate temperature improves the properties and humidity sensing performance of the ITO thin film. An annealing temperature of 600°C is suitable for enhancing the crystallinity of thin film with increased grain size. A substrate temperature maximum of 200°C is appropriate for getting an advanced property of thin films. A maximum of 10% of tin concentration is more suitable for the ITO thin film humidity sensing. The thin film's maximum thickness of 300 nm results in lower resistance and good sensitivity. Thin films' properties of low resistivity, high grain size, low bandgap, and polycrystalline structures are fundamental to obtain the highly sensitive ITO humidity sensing thin films. It is important to note that some of the preparation requires special arrangements. For example, the high deposition rate and high substrate temperatures are possible but through certain preparation methods. However, annealing, different tin concentration solutions, and varying thickness can be achieved through almost all the preparation methods.

ITO thin film sense various humidity ranges based on the measurement changes of resistance/capacitance. Thin film humidity sensitivity depends on films properties and humidity range. For example, the low resistance thin film can detect a low humidity level. Band gap minimisation and low thin film thickness enhance conductivity of the thin film and humidity sensitivity. A high humidity range shows a higher conductivity because high water molecules provide many electron donors and reduce thin film resistance. However, it is worth noting that, so far, thin film performance for humidity sensing responses is undetected at humidity levels of 5% relative humidity and below. Overall, the response and recovery times of the humidity sensing are based on the preparation method, conditions, and humidity range.

As a recommendation, ITO thin film could be a more appropriate humidity sensing element to monitor humidity in various conditions with an advanced sensor design of the two parallel plates with pores on one plate to enhance the humidity contact. It is important to consider the properties and limitations of other humidity sensing materials and optimize the range of preparation conditions to develop an improved ITO thin film for efficient humidity sensing. A better ITO humidity sensor should be compact in size to fit into confined spaces (e.g., pipeline-insulation, wall insulation interface) and exhibit improved sensitivity for monitoring even small amount humidity levels and changes. Further experimental study is needed to quantify humidity and sense the relative humidity range below 5%. The outcome of future studies could be to develop a better ITO thin film humidity sensor that can effectively monitor humidity, provide precise humidity change data, and can help with maintenance planning, prevent material failures, and mitigate economic losses.

NOMENCLATURE

d   Crystalline size
k   Shape factor

R_a	Surface height roughness
S	Sensitivity
β	Full width at half maximum
θ	Bragg's angle
λ	Wavelength of the incident beam
ρ	Resistivity
δ	Surface roughness
θ_0	Angle of incidence

AUTHOR CONTRIBUTIONS

Vinooth Rajendran: Conceptualization (lead); investigation (lead); methodology (lead); validation (lead); writing – original draft (lead). **Anil Prathuru:** Methodology (supporting); supervision (supporting); validation (supporting); writing – review and editing (supporting). **Carlos Fernandez:** Methodology (supporting); supervision (supporting); validation (supporting); writing – review and editing (supporting). **Sujatha D:** Methodology (supporting); validation (supporting); writing – review and editing (supporting). **Subhendu K. Panda:** Methodology (supporting); validation (supporting); writing – review and editing (supporting). **Nadimul Haque Faisal:** Conceptualization (lead); funding acquisition (lead); investigation (supporting); methodology (supporting); project administration (lead); supervision (lead); validation (supporting); writing – review and editing (supporting).

CONFLICT OF INTEREST STATEMENT

The authors have no conflict of interest relevant to this article.

PEER REVIEW

The peer review history for this article is available at https://www.webofscience.com/api/gateway/wos/peer-review/10.1002/eng2.12836.

DATA AVAILABILITY STATEMENT

Data sharing is not applicable to this article as no new data were created or analyzed in this study.

ORCID

Nadimul Haque Faisal https://orcid.org/0000-0001-5033-6336

REFERENCES

1. Alam MJ, Cameron DC. Optical and electrical properties of transparent conductive ITO thin films deposited by sol–gel process. *Thin Solid Films*. 2000;377:455-459. doi:10.1016/S0040-6090(00)01369-9
2. Jiao Z, Wu M, Gu J, Sun X. The gas sensing characteristics of ITO thin film prepared by sol–gel method. *Sens Actuators B*. 2003;94(2):216-221. doi:10.1016/S0925-4005(03)00343-5
3. Ota R, Seki S, Sawada Y, et al. Indium-tin-oxide films prepared by dip coating using an ethanol solution of indium chloride and tin chloride. *Surf Coat Technol*. 2003;169:521-524. doi:10.1016/S0257-8972(03)00168-3
4. Ramanan SR. Dip coated ITO thin-films through sol–gel process using metal salts. *Thin Solid Films*. 2001;389(1–2):207-212. doi:10.1016/S0040-6090(01)00825-2
5. Toki M, Aizawa M. Sol-gel formation of ITO thin film from a sol including ITO powder. *J Sol-Gel Sci Technol*. 1997;8(1):717-720. doi:10.1007/BF02436928
6. Valencia HY, Moreno LC, Ardila AM. Structural, electrical and optical analysis of ITO thin films prepared by sol–gel. *Microelectron J*. 2008;39(11):1356-1357. doi:10.1016/j.mejo.2008.01.036
7. Zamarreño CR, Hernaez M, Del Villar I, Matias IR, Arregui FJ. Tunable humidity sensor based on ITO-coated optical fiber. *Sens Actuators B*. 2010;146(1):414-417. doi:10.1016/j.snb.2010.02.029

8. Ahn MH, Cho ES, Kwon SJ. Effect of the duty ratio on the indium tin oxide (ITO) film deposited by in-line pulsed DC magnetron sputtering method for resistive touch panel. *Appl Surf Sci*. 2011;258(3):1242-1248. doi:10.1016/j.apsusc.2011.09.081

9. Askari H, Fallah H, Askari M, Mohmmadieyh MC. Electrical and optical properties of ITO thin films prepared by DC magnetron sputtering for low-emitting coatings. arXiv Preprint arXiv:1409.5293. 2014. doi:10.48550/arXiv.1409.5293

10. Chen A, Zhu K, Zhong H, Shao Q, Ge G. A new investigation of oxygen flow influence on ITO thin films by magnetron sputtering. *Sol Energy Mater Sol Cells*. 2014;120:157-162. doi:10.1016/j.solmat.2013.08.036

11. Kumar KJ, Raju NRC, Subrahmanyam A. Thickness dependent physical and photocatalytic properties of ITO thin films prepared by reactive DC magnetron sputtering. *Appl Surf Sci*. 2011;257(7):3075-3080. doi:10.1016/j.apsusc.2010.10.119

12. McGhee JR, Sagu JS, Southee DJ, Wijayantha KGU. Humidity sensing properties of transparent sputter-coated indium–tin oxide and printed polymer structures. *IEEE Sens J*. 2018;18(18):7358-7364. doi:10.1109/JSEN.2018.2858021

13. Sako T, Ohmi A, Yumoto H, Nishiyama K. ITO-film gas sensor for measuring photodecomposition of NO_2 gas. *Surf Coat Technol*. 2001;142:781-785. doi:10.1016/S0257-8972(01)01107-0

14. Teixeira V, Cui HN, Meng LJ, Fortunato E, Martins R. Amorphous ITO thin films prepared by DC sputtering for electrochromic applications. *Thin Solid Films*. 2002;420:70-75. doi:10.1016/S0040-6090(02)00656-9

15. Antony A, Nisha M, Manoj R, Jayaraj MK. Influence of target to substrate spacing on the properties of ITO thin films. *Appl Surf Sci*. 2004;225(1–4):294-301. doi:10.1016/j.apsusc.2003.10.017

16. Daza LG, Acosta M, Castro-Rodriguez R, Iribarren A. Tuning optical properties of ITO films grown by rf sputtering: effects of oblique angle deposition and thermal annealing. *Trans Nonferrous Met Soc Chin*. 2019;29(12):2566-2576. doi:10.1016/S1003-6326(19)65164-2

17. El Akkad F, Marafi M, Punnoose A, Prabu G. Effect of substrate temperature on the structural, electrical and optical properties of ITO films prepared by rf magnetron sputtering. *Phys Status Solidi (a)*. 2000;177(2):445-452. doi:10.1002/(SICI)1521-396X(200002)177:2<445::AID-PSSA445>3.0.CO;2-N

18. Ghorannevis Z, Akbarnejad E, Ghoranneviss M. Structural and morphological properties of ITO thin films grown by magnetron sputtering. *J Theor Appl Phys*. 2015;9(4):285-290. doi:10.1007/s40094-015-0187-3

19. Guillén C, Herrero J. Comparison study of ITO thin films deposited by sputtering at room temperature onto polymer and glass substrates. *Thin Solid Films*. 2005;480:129-132. doi:10.1016/j.tsf.2004.11.040

20. Herrero J, Guillen C. Improved ITO thin films for photovoltaic applications with a thin ZnO layer by sputtering. *Thin Solid Films*. 2004;451:630-633. doi:10.1016/j.tsf.2003.11.050

21. Jun SI, McKnight TE, Simpson ML, Rack PD. A statistical parameter study of indium tin oxide thin films deposited by radio-frequency sputtering. *Thin Solid Films*. 2005;476(1):59-64. doi:10.1016/j.tsf.2004.09.011

22. Nisha M, Anusha S, Antony A, Manoj R, Jayaraj MK. Effect of substrate temperature on the growth of ITO thin films. *Appl Surf Sci*. 2005;252(5):1430-1435. doi:10.1016/j.apsusc.2005.02.115

23. Sun XW, Wang LD, Kwok HS. Improved ITO thin films with a thin ZnO buffer layer by sputtering. *Thin Solid Films*. 2000;360(1–2):75-81. doi:10.1016/S0040-6090(99)01077-9

24. Wang Y, Zhang C, Li J, Ding G, Duan L. Fabrication and characterization of ITO thin film resistance temperature detector. *Vacuum*. 2017;140:121-125. doi:10.1016/j.vacuum.2016.07.028

25. Babu BM, Vadivel S. High performance humidity sensing properties of indium tin oxide (ITO) thin films by sol–gel spin coating method. *J Mater Sci Mater Electron*. 2017;28(3):2442-2447. doi:10.1007/s10854-016-5816-3

26. Cho H, Yun YH. Characterization of indium tin oxide (ITO) thin films prepared by a sol–gel spin coating process. *Ceram Int*. 2011;37(2):615-619. doi:10.1016/j.ceramint.2010.09.033

27. Dong L, Zhu GS, Xu HR, et al. Preparation of indium tin oxide (ITO) thin film with (400) preferred orientation by sol–gel spin coating method. *J Mater Sci Mater Electron*. 2019;30(8):8047-8054. doi:10.1007/s10854-019-01126-1

28. Jafan MMH, Zamani-Meymian MR, Rahimi R, Rabbani M. Effect of pyrolysis temperature on the electrical, optical, structural, and morphological properties of ITO thin films prepared by a sol–gel spin coating process. *Microelectron Eng*. 2014;130:40-45. doi:10.1016/j.mee.2014.09.009

29. Kim SS, Choi SY, Park CG, Jin HW. Transparent conductive ITO thin films through the sol-gel process using metal salts. *Thin Solid Films*. 1999;347(1–2):155-160. doi:10.1016/S0040-6090(98)01748-9

30. Majed MA, Mou SS. Synthesis and characterization of spin coated ITO films. 2017. In Proc. of International Conference on Computer, Communication, Chemical, Material and Electronic Engineering (IC4ME2–2017), Rajshahi, Bangladesh.

31. Premkumar M, Vadivel S. Effect of annealing temperature on structural, optical and humidity sensing properties of indium tin oxide (ITO) thin films. *J Mater Sci Mater Electron*. 2017;28(12):8460-8466. doi:10.1007/s10854-017-6566-6

32. Sethuraman S, Gerhardt RA. Controlling the electrical, optical, and morphological properties of sol–gel spin-coated indium tin oxide films. *AIP Adv*. 2021;11(10):105117. doi:10.1063/5.0065112

33. Sunde TOL, Garskaite E, Otter B, et al. Transparent and conducting ITO thin films by spin coating of an aqueous precursor solution. *J Mater Chem*. 2012;22(31):15740-15749. doi:10.1039/C2JM32000B

34. Yadav BC, Agrahari K, Singh S, Yadav TP. Fabrication and characterization of nanostructured indium tin oxide film and its application as humidity and gas sensors. *J Mater Sci Mater Electron*. 2016;27(5):4172-4179. doi:10.1007/s10854-016-4279-x

35. Sofi AH, Shah MA, Asokan K. Structural, optical and electrical properties of ITO thin films. *J Electron Mater*. 2018;47(2):1344-1352. doi:10.1007/s11664-017-5915-9

36. Vaishnav VS, Patel PD, Patel NG. Indium tin oxide thin film gas sensors for detection of ethanol vapours. *Thin Solid Films*. 2005;490(1):94-100. doi:10.1016/j.tsf.2005.04.006

37. Vaishnav VS, Patel SG, Panchal JN. Development of indium tin oxide thin film toluene sensor. *Sens Actuators B*. 2015;210:165-172. doi:10.1016/j.snb.2014.11.075

38. Davood R, Faegh H. Surface morphology dynamics in ITO thin films. *J Mod Phys*. 2012;2012:645-651. doi:10.4236/jmp.2012.38088

39. George J, Menon CS. Electrical and optical properties of electron beam evaporated ITO thin films. *Surf Coat Technol*. 2000;132(1):45-48. doi:10.1016/S0257-8972(00)00726-X

40. Raoufi D, Fallah HR, Kiasatpour A, Rozatian ASH. Multifractal analysis of ITO thin films prepared by electron beam deposition method. *Appl Surf Sci*. 2008;254(7):2168-2173. doi:10.1016/j.apsusc.2007.09.015

41. Raoufi D, Kiasatpour A, Fallah HR, Rozatian ASH. Surface characterization and microstructure of ITO thin films at different annealing temperatures. *Appl Surf Sci*. 2007;253(23):9085-9090. doi:10.1016/j.apsusc.2007.05.032

42. Senthilkumar V, Vickraman P, Jayachandran M, Sanjeeviraja C. Structural and optical properties of indium tin oxide (ITO) thin films with different compositions prepared by electron beam evaporation. *Vacuum*. 2010;84(6):864-869. doi:10.1016/j.vacuum.2009.11.017

43. Alyamani A, Mustapha N. Effects of high dose gamma irradiation on ITO thin film properties. *Thin Solid Films*. 2016;611:27-32. doi:10.1016/j.tsf.2016.05.022

44. Craciun V, Craciun D, Wang X, Anderson TJ, Singh RK. Highly conducting indium tin oxide films grown by ultraviolet-assisted pulsed laser deposition at low temperatures. *Thin Solid Films*. 2004;453:256-261. doi:10.1016/j.tsf.2003.11.132

45. Li H, Guo L, Liu X, et al. High temperature conductive stability of indium tin oxide films. *Front Mater*. 2020;7:113. doi:10.3389/fmats.2020.00113

46. Gaskell JM, Sheel DW. Deposition of indium tin oxide by atmospheric pressure chemical vapour deposition. *Thin Solid Films*. 2012;520(12):4110-4113. doi:10.1016/j.tsf.2011.04.191

47. Maruyama T, Fukui K. Indium tin oxide thin films prepared by chemical vapour deposition. *Thin Solid Films*. 1991;203(2):297-302. doi:10.1016/0040-6090(91)90137-M

48. Meng LJ, Placido F. Annealing effect on ITO thin films prepared by microwave-enhanced dc reactive magnetron sputtering for telecommunication applications. *Surf Coat Technol*. 2003;166(1):44-50. doi:10.1016/S0257-8972(02)00767-3

49. Okuya M, Ito N, Shiozaki K. ITO thin films prepared by a microwave heating. *Thin Solid Films*. 2007;515(24):8656-8659. doi:10.1016/j.tsf.2007.03.148

50. McGhee JR, Middlemiss RB, Southee DJ, Wijayantha KGU, Evans PS. Flexible, all metal-oxide capacitors for printed electronics. In 2018 IEEE 13th Nanotechnology Materials and Devices Conference (NMDC) (pp. 1–4). IEEE. 2018. doi:10.1109/NMDC.2018.8605872

51. Bessais B, Ezzaouia H, Bennaceur R. Electrical behaviour and optical properties of screen-printed ITO thin films. *Semicond Sci Technol*. 1993;8(8):1671-1678. doi:10.1088/0268-1242/8/8/031

52. Madhi I, Meddeb W, Bouzid B, Saadoun M, Bessaïs B. Effect of temperature and NO_2 surface adsorption on electrical properties of screen printed ITO thin film. *Appl Surf Sci*. 2015;355:242-249. doi:10.1016/j.apsusc.2015.07.135

53. Mbarek H, Saadoun M, Bessais B. Screen-printed tin-doped indium oxide (ITO) films for NH3 gas sensing. *Mater Sci Eng C*. 2006;26(2–3):500-504. doi:10.1016/j.msec.2005.10.037

54. McGhee JR, Sagu JS, Southee DJ, Evans PS, Wijayantha KU. Printed, fully metal oxide, capacitive humidity sensors using conductive indium tin oxide inks. *ACS Appl Electron Mater*. 2020;2(11):3593-3600. doi:10.1021/acsaelm.0c00660

55. Qiao F, Lu L, Han P, et al. A combined experimental and theoretical study of screen-printing high transparent conductive mesoscopic ito films. *Sci Rep*. 2020;10(1):1-11. doi:10.1038/s41598-020-61124-w

56. Tian B, Cheng G, Zhang Z, et al. Optimization on thermoelectric characteristics of indium tin oxide/indium oxide thin film thermocouples based on screen printing technology. *Rev Sci Instrum*. 2021;92(10):105001. doi:10.1063/5.0057148

57. Keshmiri SH, Rezaee-Roknabadi M, Ashok S. A novel technique for increasing electron mobility of indium-tin-oxide transparent conducting films. *Thin Solid Films*. 2002;413(1–2):167-170. doi:10.1016/S0040-6090(02)00340-1

58. Marikkannu S, Kashif M, Sethupathy N, et al. Effect of substrate temperature on indium tin oxide (ITO) thin films deposited by jet nebulizer spray pyrolysis and solar cell application. *Mater Sci Semicond Process*. 2014;27:562-568. doi:10.1016/j.mssp.2014.07.036

59. Moholkar AV, Pawar SM, Rajpure KY, Ganesan V, Bhosale CH. Effect of precursor concentration on the properties of ITO thin films. *J Alloys Compd*. 2008;464(1–2):387-392. doi:10.1016/j.jallcom.2007.09.138

60. Hwang DK, Misra M, Lee YE, Baek SD, Myoung JM, Lee TI. The role of Ar plasma treatment in generating oxygen vacancies in indium tin oxide thin films prepared by the sol-gel process. *Appl Surf Sci*. 2017;405:344-349. doi:10.1016/j.apsusc.2017.02.007

61. Salehi A. The effects of deposition rate and substrate temperature of ITO thin films on electrical and optical properties. *Thin Solid Films*. 1998;324(1–2):214-218. doi:10.1016/S0040-6090(98)00371-X

62. Hoshi Y, Kato HO, Funatsu K. Structure and electrical properties of ITO thin films deposited at high rate by facing target sputtering. *Thin Solid Films*. 2003;445(2):245-250. doi:10.1016/S0040-6090(03)01182-9

63. Liu Z, Liang J, Zhou H, et al. Effect of nitrogen partial pressure on the TCR of magnetron sputtered indium tin oxide thin films at high temperatures. *Ceram Int*. 2022;48(9):12924-12931. doi:10.1016/j.ceramint.2022.01.165

64. Cho H, Tamura Y, Matsuo T. Monitoring of corrosion under insulations by acoustic emission and humidity measurement. *J Nondestruct Eval*. 2011;30(2):59-63. doi:10.1007/s10921-011-0090-z

65. Delipinar T, Shafique A, Gohar MS, Yapici MK. Fabrication and materials integration of flexible humidity sensors for emerging applications. *ACS Omega*. 2021;6(13):8744-8753. doi:10.1021/acsomega.0c06106

66. Harpster TJ, Stark B, Najafi K. A passive wireless integrated humidity sensor. *Sens Actuators A Phys*. 2002;95(2–3):100-107. doi:10.1016/S0924-4247(01)00720-8

67. Kapic A, Tsirou A, Verdini PG, Carrara S. Humidity sensors for high energy physics applications: a review. *IEEE Sens J*. 2020;20(18):10335-10344. doi:10.1109/JSEN.2020.2994315

68. He P, Brent JR, Ding H, et al. Fully printed high performance humidity sensors based on two-dimensional materials. *Nanoscale*. 2018;10(12):5599-5606. doi:10.1039/C7NR08115D

69. Sehrawat P, Islam SS, Mishra P, Ahmad S. Reduced graphene oxide (rGO) based wideband optical sensor and the role of temperature, defect states and quantum efficiency. *Sci Rep*. 2018;8(1):1-13. doi:10.1038/s41598-018-21686-2

70. Kolodziejczak-radzimska A, Jesionowski T. Zinc oxide—from synthesis to application: a review. *Materials*. 2014;7(4):2833-2881. doi:10.3390/ma7042833

71. Yawale SP, Yawale SS, Lamdhade GT. Tin oxide and zinc oxide based doped humidity sensors. *Sens Actuators A Phys*. 2007;135(2):388-393. doi:10.1016/j.sna.2006.08.001

72. Vinnik IB, Uvarova IV, Zenkov VS. Ceramic humidity sensors based on zirconium dioxide. *Powder Metall Met Ceram*. 1998;37(11):632-634.

73. Wang Z, Lu Y, Yuan S, et al. Hydrothermal synthesis and humidity sensing properties of size-controlled zirconium oxide (ZrO2) nanorods. *J Colloid Interface Sci*. 2013;396:9-15. doi:10.1016/j.jcis.2012.12.068

74. Agool IR, Kadhim KJ, Hashim A. Fabrication of new nanocomposites: (PVA-PEG-PVP) blend-zirconium oxide nanoparticles for humidity sensors. *Int J Plastics Technol*. 2017;21(2):397-403. doi:10.1007/s12588-017-9192-5

75. Sathya P. Design and development of thin film humidity sensor based on alumina and zirconium dioxide. In 2020 International Conference on Emerging Trends in Information Technology and Engineering (Ic-ETITE) (pp. 1–5). IEEE. 2020. doi:10.1109/ic-ETITE47903.2020.270

76. Renukadevi R, Sundaram R, Kasinathan K. Barium oxide nanoparticles with robust catalytic, photocatalytic and humidity sensing properties. *J Nanostruct*. 2020;10(1):167-176. doi:10.22052/JNS.2020.01.018

77. Pascariu P, Airinei A, Olaru N, et al. Microstructure, electrical and humidity sensor properties of electrospun NiO–SnO2 nanofibers. *Sens Actuators B*. 2016;222:1024-1031. doi:10.1016/j.snb.2015.09.051

78. Parthibavarman M, Hariharan V, Sekar CJMS. High-sensitivity humidity sensor based on SnO2 nanoparticles synthesized by microwave irradiation method. *Mater Sci Eng C*. 2011;31(5):840-844. doi:10.1016/j.msec.2011.01.002

79. Li F, Li P, Zhang H. Preparation and research of a high-performance ZnO/SnO2 humidity sensor. *Sensors*. 2021;22(1):293. doi:10.3390/s22010293

80. Nishio K, Sei T, Tsuchiya T. Preparation and electrical properties of ITO thin films by dip-coating process. *J Mater Sci*. 1996;31(7):1761-1766. doi:10.1007/BF00372189

81. Almeida JB. Design of magnetrons for dc sputtering. *Vacuum*. 1989;39(7–8):717-721. doi:10.1016/0042-207X(89)90023-7

82. Su C, Sheu TK, Chang YT, Wan MA, Feng MC, Hung WC. Preparation of ITO thin films by sol-gel process and their characterizations. *Synth Met*. 2005;153(1–3):9-12. doi:10.1016/j.synthmet.2005.07.219

83. Singh A, Kumar K, Sikarwar S, Yadav BC. Highly sensitive and selective LPG sensor working below lowest explosion limit (LEL) at room temperature using as-fabricated indium doped SnO2 thin film. *Mater Chem Phys*. 2022;287:126275. doi:10.1016/j.matchemphys.2022.126275

84. Patel NG, Makhija KK, Panchal CJ. Fabrication of carbon dioxide gas sensor and its alarm system using indium tin oxide (ITO) thin films. *Sens Actuators B*. 1994;21(3):193-197. doi:10.1016/0925-4005(94)01247-4

85. Kim H, Horwitz JS, Pique A, Gilmore CM, Chrisey DB. Electrical and optical properties of indium tin oxide thin films grown by pulsed laser deposition. *Appl Phys A*. 1999;69(1):S447-S450. doi:10.1007/s003390051435

86. Siddiqui MS, Saxena AK, Singh SP. Deposition and characterization of ITO thin film over glass for defogger application and for solar photovoltaics. *Int J Curr Eng Technol*. 2018;8:4-8. doi:10.14741/ijcet/v.8.4.1

87. Benamar E, Rami M, Messaoudi C, Sayah D, Ennaoui A. Structural, optical and electrical properties of indium tin oxide thin films prepared by spray pyrolysis. *Solar Energy Mater Solar Cells*. 1999;56(2):125-139. doi:10.1016/S0927-0248(98)00151-2

88. Fereidooni M, Márquez V, Paz CV, et al. On the CO$_2$ photocatalytic reduction over indium tin oxide (ITO) ultra-thin films in water vapor: experimental and theoretical study. *Fuel*. 2023;349:128652. doi:10.1016/j.fuel.2023.128652

89. Kerkache L, Layadi A, Dogheche E, Remiens D. Structural, ferroelectric and dielectric properties of In2O3: Sn (ITO) on PbZr0. 53Ti0. 47O3 (PZT)/Pt and annealing effect. *J Alloys Compd*. 2011;509(20):6072-6076. doi:10.1016/j.jallcom.2011.03.022

90. Tang W, Chao Y, Weng X, Deng L, Xu K. Optical property and the relationship between resistivity and surface roughness of indium tin oxide thin films. *Phys Proc*. 2012;32:680-686. doi:10.1016/j.phpro.2012.03.618

91. Lee JH, Kim YH, Ahn SJ, Ha TH, Kim HS. Grain-size effect on the electrical properties of nanocrystalline indium tin oxide thin films. *Mater Sci Eng B*. 2015;199:37-41. doi:10.1016/j.mseb.2015.04.011

92. Beaurain A, Luxembourg D, Dufour C, Koncar V, Capoen B, Bouazaoui M. Effects of annealing temperature and heat-treatment duration on electrical properties of sol–gel derived indium-tin-oxide thin films. *Thin Solid Films*. 2008;516(12):4102-4106. doi:10.1016/j.tsf.2007.10.021

93. Alyamani A, Mustapha N, Alkhuraiji TS, Idriss H. Influence of gamma ray and thermal annealing on zinc oxide and titanium oxide thin films characteristics. *J Ovon Res*. 2019;15(5):301-313.

94. Cui HN, Teixeira V, Meng LJ, Martins R, Fortunato E. Influence of oxygen/argon pressure ratio on the morphology, optical and electrical properties of ITO thin films deposited at room temperature. *Vacuum*. 2008;82(12):1507-1511. doi:10.1016/j.vacuum.2008.03.061

95. Sangwaranatee N, Srithanachai I. Preparation and investigation indium tin oxide for transparent electrode of MS Schottky photodiode. In Journal of Physics: Conference Series (Vol 2331, No 1, p 012007). IOP Publishing. 2022. doi:10.1088/1742-6596/2331/1/012007

96. Lian J, Zhang D, Hong R, Qiu P, Lv T, Zhang D. Defect-induced tunable permittivity of epsilon-near-zero in indium tin oxide thin films. *Nanomaterials*. 2018;8(11):922. doi:10.3390/nano8110922

97. Hong R, Yan T, Tao C, Wang Q, Lin H, Zhang D. Laser induced the tunable permittivity of epsilon-near-zero induced in indium tin oxide thin films. *Opt Mater*. 2020;107:110137. doi:10.1016/j.optmat.2020.110137

98. Al-Kuhaili MF. Electrical conductivity enhancement of indium tin oxide (ITO) thin films reactively sputtered in a hydrogen plasma. *J Mater Sci Mater Electron*. 2020;31(4):2729-2740. doi:10.1007/s10854-019-02813-9

99. Hsu CH, Zhang ZX, Shi CY, et al. Single-crystalline-like indium tin oxide thin films prepared by plasma enhanced atomic layer deposition. *J Mater Chem C*. 2022;10(34):12350-12358. doi:10.1039/D2TC01834A

100. Kuzubasoglu BA. Recent studies on the humidity sensor: a mini review. *ACS Appl Electron Mater*. 2022;4(10):4797-4807. doi:10.1021/acsaelm.2c00721

101. Lakshmi RB, Juliet AV. Effect of annealing on humidity sensing properties of Sm-doped SnO_2 thin films. *J Mater Res Technol*. 2019;8(6):5862-5866. doi:10.1016/j.jmrt.2019.09.057

102. Mallick S, Ahmad Z, Touati F, Bhadra J, Shakoor RA, Al-Thani NJ. PLA-TiO_2 nanocomposites: thermal, morphological, structural, and humidity sensing properties. *Ceram Int*. 2018;44(14):16507-16513. doi:10.1016/j.ceramint.2018.06.068

103. Sajid M, Khattak ZJ, Rahman K, Hassan G, Choi KH. Progress and future of relative humidity sensors: a review from materials perspective. *Bull Mater Sci*. 2022;45(4):238. doi:10.1007/s12034-022-02799-x

104. Oh SJ, Kwon JH, Lee S, Choi KC, Kim TS. Unveiling the annealing-dependent mechanical properties of freestanding indium tin oxide thin films. *ACS Appl Mater Interfaces*. 2021;13(14):16650-16659. doi:10.1021/acsami.0c23112

105. Rao T, Li J, Cai W, et al. Fabrication of a mesoporous multimetallic oxide-based ion-sensitive field effect transistor for pH sensing. *ACS Omega*. 2021;6(47):32297-32303. doi:10.1021/acsomega.1c05469

106. Alsultany FH, Alhasan SFH, Salim ET. Seed layer-assisted chemical bath deposition of Cu_2O nanoparticles on ITO-coated glass substrates with tunable morphology, crystallinity, and optical properties. *J Inorg Organomet Polym Mater*. 2021;31(9):3749-3759. doi:10.1007/s10904-021-02016-y

107. Saleem MS, Hanif MB, Gregor M, Motola M, Khan AF. Nanostructured multi-layer MgF_2/ITO coatings prepared via e-beam evaporation for efficient electromagnetic interference shielding performance. *Appl Surf Sci*. 2022;596:153584. doi:10.1016/j.apsusc.2022.153584

108. Song J, Huang J, Qiu L. Enhancing the adhesion strength of ink-jet printed indium tin oxide films: the role of printing parameters. *Mater Design*. 2023;232:112140. doi:10.1016/j.matdes.2023.112140

AUTHOR BIOGRAPHIES

Vinooth Rajendran is a PhD research student working on the research related to sensor design and sensor-based corrosion monitoring and analysis at Robert Gordon University, Aberdeen, UK. He obtained a Master's (Materials Science and Engineering) and Bachelor's (Chemical and Electrochemical Engineering) from Queen's University Belfast, UK, and CSIR – Central Electrochemical Research Institute, Karaikudi, India, respectively. He has experience in the Oil and Gas industry as a cathodic protection engineer for four years and a member of the Institute of Corrosion. He is currently working as a part of various teaching/research assistantships at Robert Gordon University.

Anil Prathuru is a Lecturer (Mechanical Engineering) at the School of Engineering, Robert Gordon University, an early career researcher with experience in thermal spray coating development and characterization. Before joining RGU, he worked as a mechanical engineer for EC-OG, Aberdeen, a subsea renewables company. His research interests include thermal spray coatings for energy harvesting, hydrogen energy and remote sensing applications, application of machine learning in material development. He also worked on the development of structural health monitoring based on NDT techniques and associated data processing methods. He has worked on several commercial projects related to early-stage technology development as research projects on the digitalization of material development.

Carlos Fernandez is a Senior Lecturer in Analytical Biochemistry at Robert Gordon University, Aberdeen, UK. CF has published over 150 (h = 32 Scopus, 4007 Citations Scopus) peer review articles in Analytical Chemistry (Electrochemistry) and Materials Chemistry and 20 peer review conference manuscripts. His research interests focus on the use of Materials Chemistry for Energy Storage Devices and Battery Applications and concentrate on the utilization of voltammetric techniques in Analytical Chemistry as an electrochemical sensor. CF has successfully secured as principal or co-investigator from a variety of organizations, including Oil and Gas Innovation Centre, Standard Voucher Scheme (Scottish Funding Council/Interface), Analytical Chemistry Trust

Fund, PhD studentship and Game Changers in Collaboration with NNL (National Nuclear Laboratory), and Royal Society of Edinburgh. He holds membership of several professional bodies including The Institute of Physics (MInstP), Royal Society of Chemistry (MRSC) and Electrochemical Society (MECS), and Fellow of The Royal Geographical Society (FRGS). CF is also Chartered in Chemistry (CChem), a Chartered Scientist (CCci), and a Fellow of The Higher Education Academy (FHEA).

Dhavamani Sujatha is a researcher at India's CSIR – Central Electrochemical Research Institute (CECRI). She obtained a Master's (Physical Sciences) degree from Alagappa University, India. Her research interest includes thin film battery, electrochemistry, carbon materials, sodium-ion batteries, and biofilm.

Subhendu K. Panda is a Principal Scientist at India's CSIR – Central Electrochemical Research Institute (CECRI). His research interest includes nanoscience and materials chemistry, colloidal synthesis, and studies on photo-physical properties of semiconductor nanostructures. Applications in the fields of solar cells, LEDs, sensors, fuel cells, and electrochemical energy conversion as photo/electrocatalyst for water splitting and energy storage such as batteries and supercapacitors.

Nadimul Haque Faisal (PhD, CEng, MIMechE, MIMMM, FHEA) is a Professor of Surface Engineering & Micromechanics at Robert Gordon University. His interest includes micromechanical behavior analysis of thermal spray coatings and thin films, metamaterial manufacturing using thermal spray coating techniques, sensor-based instrumented mechanical testing, and acoustic emission (AE) sensor-based condition monitoring. He has over 75 peer-reviewed journals, 1 US Patent, and 4 book chapters, and over 50 conference publications. He is member of Royal Society of Edinburgh's Young Academy of Scotland, EPSRC peer review College member, and member of UK's Metamaterials Network. Total research and commercial funding obtained is over £1.25 M (as PI/Co-I). He is Principal Investigator of recently funded EPSRC grant "METASIS" (EP/W033178/1).